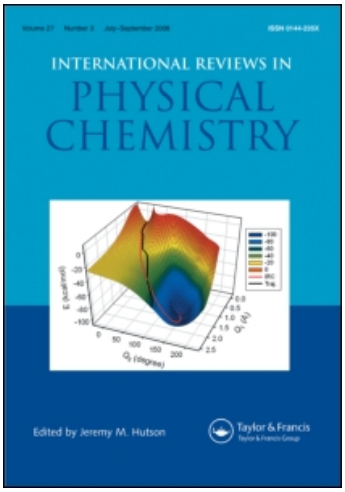

International Reviews in Physical Chemistry
Publication details, including instructions for authors and subscription information:
http://www.informaworld.com/smpp/title~content=t713724383

Time-resolved infrared-ultraviolet double-resonance spectroscopy of formaldehyde-d_2

Brian J. Orr[a]
[a] School of Chemistry, Macquarie University, New South Wales, Australia

To cite this Article Orr, Brian J.(1990) 'Time-resolved infrared-ultraviolet double-resonance spectroscopy of formaldehyde-d_2', International Reviews in Physical Chemistry, 9: 1, 67 — 113
To link to this Article: DOI: 10.1080/01442359009353238
URL: http://dx.doi.org/10.1080/01442359009353238

INTERNATIONAL REVIEWS IN PHYSICAL CHEMISTRY, 1990, VOL. 9, NO. 1, 67–113

Time-resolved infrared–ultraviolet double-resonance spectroscopy of formaldehyde-d_2

by BRIAN J. ORR
School of Chemistry, Macquarie University,
New South Wales 2109, Australia

This review concentrates on a time-resolved infrared–ultraviolet double-resonance technique which has revealed many aspects of spectroscopic properties and energy-transfer processes involving the formaldehyde-d_2 molecule, D_2CO. The experiments comprise sequential pulsed excitation of D_2CO by CO_2 and dye lasers, with visible-fluorescence detection. The infrared PUMP laser excites a transition in the ν_4, ν_6 or $(2\nu_4-\nu_4)$ vibrational band, which prepares D_2CO in a specific rovibrational quantum state. This is followed by rovibronic excitation by a tunable PROBE laser, *via* the 4_1^0, 6_1^0 or 4_2^1 *vibronic band in the* $\tilde{A}\leftarrow\tilde{X}$ *electronic absorption* system of D_2CO. Detailed spectroscopic information is obtained by keeping the product of sample pressure and PUMP–PROBE delay as small as possible (typically below 10 ns Torr), approaching collision-free conditions. Additional information on a range of collision-induced state-to-state energy transfer processes is obtained by varying the number of collisions experienced by the D_2CO molecule in the interval between the PUMP and PROBE pulses. The following kinetic and mechanistic applications are reviewed: *J*-changing rotational relaxation arising from long-range molecular interactions; mode-to-mode vibrational energy transfer, with particular emphasis on the role of rotational energy states and intramolecular perturbations; the way in which collision-induced molecular processes may be modified by selecting the rovibrational quantum state of the formaldehyde molecule and by varying its collision partner; and infrared multiple-photon excitation and laser photochemistry.

1. Introduction

The review concerns a single experimental technique and a single molecule. The technique is that of time-resolved infrared–ultraviolet double-resonance (IRUVDR) spectroscopy and the molecule is formaldehyde (H_2CO), or, more explicitly, its fully deuterated modification, D_2CO. This combination of technique and molecule has, over the last decade, provided a rich source of information on molecular behaviour. Such information ranges over a number of fields of interest to physical chemists: high-resolution molecular spectroscopy (rotational, vibrational and electronic); rotational relaxation arising from long-range molecular interactions; mode-to-mode vibrational energy transfer, with particular emphasis on the role of rotational energy states and intramolecular perturbations; the way in which collision-induced molecular processes may be modified by selecting the rovibrational quantum state of the formaldehyde molecule and by varying its collision partner; applications in the area of infrared laser photochemistry in small polyatomic molecules, with relevance to the nature of state-selective 'multiphoton' (or incoherent multiple-photon) excitation processes.

The period over which this research has been conducted has seen dramatic development in laser devices and associated detection and computational equipment, as well as a maturing of our appreciation (both experimental and theoretical) of spectroscopic and energy-transfer processes in small polyatomic molecules. The review

0144-235X/90 $3·00

is written in a style which is at times anecdotal and intended to portray the sequence in which the story has actually evolved. Such an approach may therefore contain less of the logical hindsight which characterizes much of the scientific literature and which tends to conceal the mystery, challenge and excitement of research as it progresses.

2. The IRUVDR technique

An excellent early review by Steinfeld and Houston (1978) shows that optical double-resonance spectroscopy has long been established as a sensitive means of studying molecular relaxation and photochemical processes, as well as characterizing rotational structure in molecular spectra. Of the various combinations of ultraviolet, visible, infrared, microwave and radiofrequency radiation which can be used in double-resonance spectroscopy, infrared–ultraviolet double-resonance (IRUVDR) was a relatively late developer (Steinfeld and Houston 1978) and, even now, comparatively few examples of IRUVDR have been sufficiently selective to enable molecular rotational structure to be clearly resolved.

A simplified diagram of the three-level IRUVDR excitation scheme used in our studies of D_2CO is shown in figure 1 (Orr and Nutt 1980a, b). Infrared excitation (**1**←**0**) by a PUMP pulse from a monochromatic CO_2 laser produces an instantaneous population increase in the single rovibrational level **1**. Subsequent collisions enabling rotational relaxation to adjacent levels cause that selective population increase to be rapidly depleted, at a rate which is typically an order of magnitude faster than that of gas-kinetic collisions. It is therefore necessary that the second step in the IRUVDR scheme of figure 1, rovibronic PROBE excitation (**2**←**1**), should follow that PUMP excitation (**1**←**0**) by an accurately controlled interval short enough to avoid significant population depletion by rotational relaxation (Orr and Nutt 1980a). In our

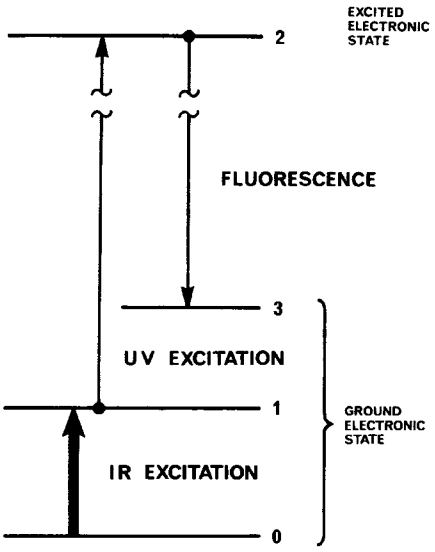

Figure 1. Excitation scheme for infrared–ultraviolet double-resonance (IRUVDR). Levels **0** and **1** are specific rovibrational levels of the ground electronic state and level **2** belongs to an excited vibronic state of the molecule. The IR and UV excitation steps (**1**←**0** and **2**←**1**) are referred to as the PUMP and PROBE steps respectively. They are separated in time by a short IR–UV delay. Note that the fluorescence transition **2**→**3** generally occurs after relaxation within the excited electronic state (Orr and Nutt 1980a, b).

experiments this PROBE excitation is produced by a pulsed tunable dye laser operating in the near-ultraviolet region, the IR–UV delay between PUMP and PROBE pulses typically being in the sub-microsecond range for sample pressures of approximately 100 mTorr. The infrared PUMP and ultraviolet PROBE radiation therefore combine efficiently to produce a selective stepwise excitation of the rovibrational level **1** and of the rovibronic level **2** only if the lasers are in resonance with the respective transitions and if the PROBE pulse follows the PUMP pulse by an IR–UV delay shorter than the rotational relaxation time of level **1**. The rigour of these resonance and timing conditions determines the high sensitivity and selectivity of the optical double resonance technique. In our IRUVDR scheme the occurrence of a double resonance is detected by viewing laser-induced fluorescence (LIF) from the vibronic state excited by the two-step process. In general the optical emission process (labelled **2**→**3** in figure 1) will occur after rotational, and sometimes vibrational, relaxation of the population of the excited level **2**, so that a fully structured rovibronic emission spectrum results, with its intensity distribution determined by the Franck–Condon principle. One particular advantage of the IRUVDR technique is that the spectroscopic assignment and relaxation behaviour of a specific molecular rovibrational level, directly accessible by infrared spectroscopy, may be monitored in the visible/ultraviolet region where detector sensitivity and time response are in general superior to that in the infrared. For a given infrared excitation process **1**←**0** there will in general be several corresponding rovibronic transitions **2**←**1** which may be excited by the tunable ultraviolet radiation; the resulting spectroscopic pattern is useful as a means of identifying the rovibrational level **1** excited by the PUMP radiation.

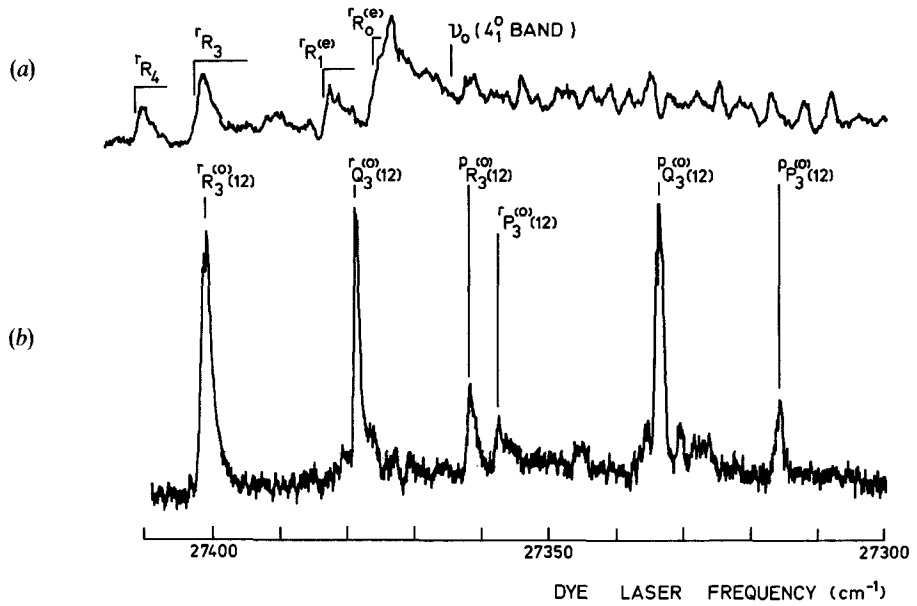

Figure 2. (*a*) Background LIF excitation spectrum of the 365 nm 4_1^0 band of D_2CO, with vibronic band origin and prominent $^{r}R_K$ sub-band heads marked. (*b*) IRUVDR difference spectrum for D_2CO pumped by the 10·55 μm 10 P(16) line of a CO_2 laser (pulse energy, 0·4 J; beam area, 0·5 cm^2; IR–UV delay, 0·5 μs). The detection sensitivity and frequency scale are common to both spectra (*a*) and (*b*), as are the D_2CO pressure (5 mTorr) and dye laser bandwidth ($\sim$1 cm^{-1}). See figure 3 and section 4 for further explanation of spectroscopic assignments and notation (Orr and Nutt 1980*b*).

An illustrative example of a rotationally resolved IRUVDR spectrum is shown in figure 2(*b*) (Orr and Nutt 1980b). Above it, in figure 2(*a*), is the corresponding LIF excitation spectrum of the 365 nm 4_1^0 hot band in the $\tilde{A}\leftarrow\tilde{X}$ electronic absorption system of D_2CO. The rovibrational PUMP transition is that coinciding with the 10·55 μm 10 P(16) CO_2 laser line, which excites a single rovibrational transition in the ν_4 infrared band of D_2CO. All six allowed rovibronic PROBE transitions emanating from the selected rovibrational level are clearly displayed in the resulting IRUVDR spectrum of the 4_1^0 band (figure 2(*b*)), recorded as the difference between LIF excitation spectra recorded with IR PUMP radiation on and off. The IRUVDR peaks show a 50-fold enhancement with respect to the background spectrum (figure 2(*a*)), indicating saturation of the rovibrational transition by the CO_2 laser. The product of IR–UV delay and pressure in this example is $\sim$2·5 ns Torr, which corresponds to a collision number z of 0·025 (based on a hard-sphere collision diameter of 4·0 Å for D_2CO) and hence to effectively collision-free conditions.

The spectroscopic assignment of the IRUVDR process described in the preceding paragraph is illustrated in figure 3. This serves also to introduce some standard molecular spectroscopic notation, which may not be familar to all readers. More detailed explanations are available in section 4, but the mystique of spectroscopic notation should in the meantime not be allowed to obscure the fundamental physical processes of interest.

The ability of the IRUVDR technique to simplify congested rotational structure in molecular spectra is further demonstrated by figure 4 (Orr and Haub 1984). This shows a portion of the infrared absorption spectrum of D_2CO in the region which contains the 10 P(16) CO_2 laser line used to generate the IRUVDR spectrum of figure 2(*b*). Despite the relatively high spectroscopic resolution, the rovibrational transition excited by the CO_2 laser line is not clearly discernible, because the ν_4 vibrational band to which it belongs is overlapped by the more intense ν_6 band.

The main spectroscopic advantage of the IRUVDR technique therefore lies in its ability to project a correlated set of transitions (usually comprising six spectral features, all satisfying the double-resonance selection rules) out of an otherwise highly congested rovibronic spectrum. This set of rovibronic features can be analyzed in terms of upper-state combination differences to yield unambiguous assignments of the sequence of rovibrational and rovibronic transitions involved in a given IRUVDR process, even with the PROBE resolution as poor as $\sim$1 cm^{-1}. This is not only an aid in assigning congested molecular spectra, but (as we shall see) also the source of many interesting state-selected energy transfer possibilities.

3. How it all began

The IRUVDR technique of interest was first reported ten years ago by Orr and Nutt (1980a). However, what the literature does not show is that IRUVDR in D_2CO actually had its origins a further ten years before that, in a series of unreported and seemingly unproductive experiments conducted at the National Research Council of Canada (NRCC) in Ottawa by F. Legay, B. J. Orr and D. A. Ramsay (1969, unpublished results). These were performed in the early days of optical double-resonance spectroscopy (Steinfeld and Houston 1978), at a time when conventional longitudinal-discharge (both c.w. and Q-switched) CO_2 lasers were still a curiosity, when high-power, transversely excited pulsed CO_2 lasers remained a military secret, and when Hänsch's (1972) development of the tunable dye laser as a useful tool for high-resolution spectroscopy was still unrealized. High resolution in optical spectroscopy

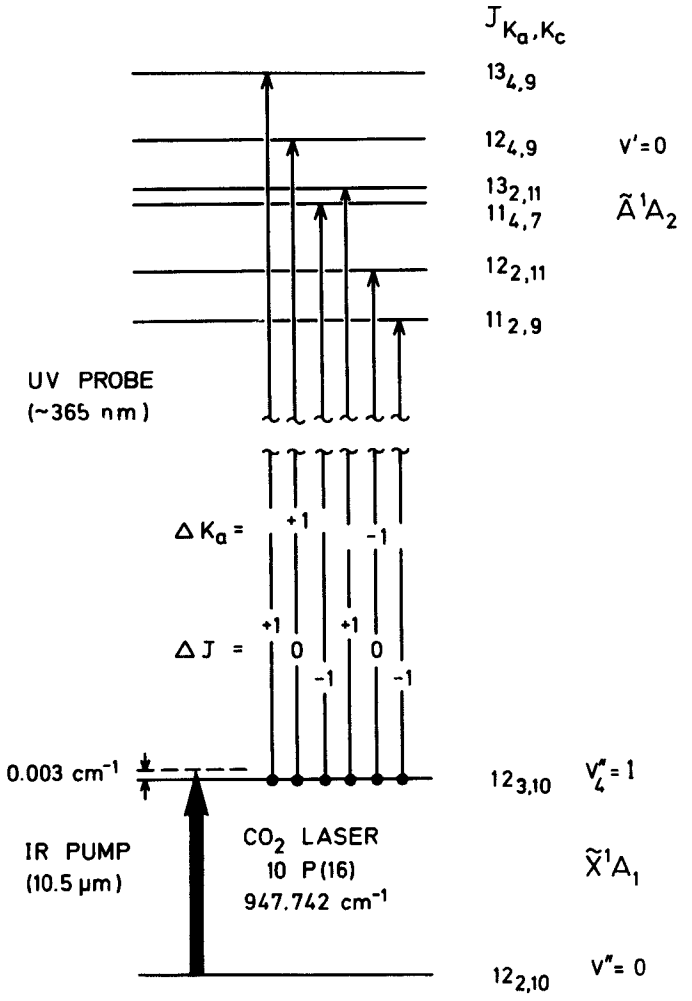

Figure 3. Detailed IRUVDR excitation scheme for D_2CO pumped by the 10 P(16) CO_2-laser line. The CO_2 laser excites the $^rQ_2^{(e)}(12)$ rotational transition in the ν_4 vibrational band of D_2CO, preparing molecules in the $J_{K_a,K_c} = 12_{3,10}$ rotational state of the $v_4'' = 1$ vibrational level. There are then six possible rotational transitions in the corresponding $\tilde{A} \leftarrow \tilde{X}$ 4_1^0 vibronic hot band used to probe that rovibrational excitation: ^rR, ^rQ and ^rP (corresponding to $\Delta J = +1, 0$ and -1 with $\Delta K_a = +1$) and ^pR, ^pQ, ^pP (corresponding to $\Delta J = +1$, 0 and -1 with $\Delta K_a = -1$); features due to these six transitions comprise the IRUVDR spectrum in figure 2 (*b*). The superscripts (e) and (o) used occasionally to label rotational transitions indicate that the sum of quantum numbers $(J'' + K_a'' + K_c'')$ for the lower level in the transition is even or odd respectively.

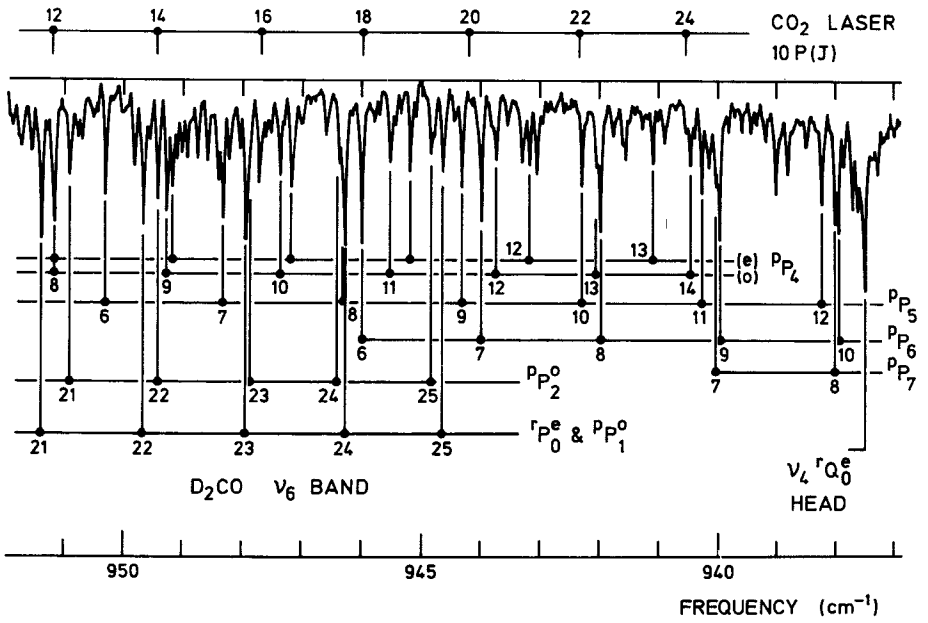

Figure 4. Infrared absorption spectrum of D_2CO vapour, recorded with a resolution of $\sim 0{\cdot}05\,cm^{-1}$ (Orr and Haub 1984). The section of spectrum shown is on the immediate high-frequency side of the ν_4-band centre and is dominated by the rovibrational structure of the ν_6 band, as shown by the assignment grids. The frequencies of the CO_2-laser lines 10 P(12)–10 P(24) are also shown; these yield assigned IRUVDR excitation in various transitions of the ν_4 and ν_6 bands (Orr and Haub 1984).

was almost invariably achieved by large grating spectrographs and the analysis of their output was (and still is) a highly developed art (Herzberg 1966). The double-resonance approach offered to high-resolution optical spectroscopists the prospect of 'tagging' particular features, associated with transitions sharing a common energy level, in a complicated and congested rovibronic spectrum. It was this quest for an aid to spectroscopic analysis that prompted us in 1969 to see whether a CO_2 laser could usefully perturb the intensity distribution of the rovibronic spectrum of a small polyatomic molecule. D_2CO was chosen as an ideal molecular candidate at an early stage, in view of its known infrared spectrum in the CO_2-laser region (Ebers and Nielsen 1938), and its well established electronic spectroscopy (Brand 1956). Initial fruitless experiments involved shining the beam from a c.w. CO_2 laser beam down a long-path cell containing D_2CO vapour, while photographically recording its absorption spectrum in the 365 nm region on a 7·3 m Ebert spectrograph over several hours. We were effectively looking for a rovibrationally selective means of enhancing hot-band features, but had naively overlooked the fact that collision-induced energy transfer would cause any selectivity to be lost in a steady-state experiment such as this.

After that early setback we decided to adopt a time-resolved approach, to abandon high spectroscopic resolution for the time being, and to employ fluorescence as a means of detection. (I believe that the fluorescence approach was first suggested to us by Dr Sidney Leach on a visit to Ottawa. Moreover, I recall being reassured in the NRCC cafeteria by Dr Gerhard Herzberg that he had observed the strong fluorescence spectrum of D_2CO with his own eyes, some time back in the 1930s! Stimulating

exchanges with experienced colleagues often pass unreported in the scientific literature.) Our apparatus comprised a 10 cm gas cell containing D_2CO vapour (typically at 30 Torr and 80°C), a 1600 W xenon lamp filtered by a variety of near-ultraviolet bandpass filters as PROBE light source, and a 50 W c.w. CO_2 laser equipped with a NaCl-prism wavelength selector as the PUMP source. The infrared laser beam was mechanically chopped at rates ranging from 200 to 2000 Hz. Visible fluorescence was viewed through selected interference filters by a photomultiplier and electronic signals processed by a lock-in amplifier. We observed two different forms of signal, depending on the combination of PROBE and fluorescence wavelengths employed. The first form of signal was modulated *in phase* with the chopped PUMP radiation; this occurred with near-ultraviolet PROBE radiation (360–400 nm), which enabled absorption of D_2CO to occur only through vibronic hot bands originating in vibrationally excited levels of the lower electronic state. The second form of signal was modulated *180° out of phase* with the PUMP and was observed with a broader range of ultraviolet PROBE wavelengths (240–400 nm) than in the previous case; these conditions allowed vibronic absorption from the $v=0$ vibrational level of D_2CO, as well as from excited vibrational levels. The sense of the in-phase signals suggested an infrared enhancement of vibronic hot-band intensity, as subsequently demonstrated in the $\nu_4/4_1^0$ IRUVDR excitation scheme observed by Orr and Nutt (1980a, b) ten years later. Likewise, the sense of the out-of-phase signals was consistent with an infrared-induced depletion of population in the vibrational ground state. However, the magnitude of the observed modulated signals (which comprised about 0·5% of total fluorescence) was too great to be attributable to a geniuine double-resonance effect. This was confirmed by further experiments which varied the PUMP wavelength and chopping rate, as well as the PROBE wavelength. The observations were therefore attributed by Legay *et al.* (1969) to a variety of thermal processes and one of us was prompted to comment that the principal message of the work was merely that 'gases get hot when exposed to an infrared laser!'—a fitting epitaph.

These early attempts to establish IRUVDR as a useful spectroscopic technique was not entirely fruitless, for they identified D_2CO as an ideal molecule for such studies, generated a body of infrared and ultraviolet spectroscopic data as a resource for future work, highlighted energy transfer processes as a crucial ingredient of any sequential excitation scheme and created a desire and determination to realize the potential of the IRUVDR technique. In particular, high-resolution rovibronic absorption spectra of the 365 nm 4_1^0 band of D_2CO vapour which had been recorded at NRCC Ottawa were duly analyzed, taking into account the strong Coriolis coupling between the ν_4 and ν_6 vibrational modes (Orr 1974). Less comprehensive analyses were also made of high-resolution infrared absorption spectra of D_2CO, recorded at NRCC in the 10 μm region, but these were never published. These spectroscopic data proved invaluable as a guide in subsequent IRUVDR studies of D_2CO.

The 1970s saw a dramatic growth in the availability of reliable laser sources and other instrumentation, accompanied by an associated revolution in molecular spectroscopy. My own laboratory at the University of New South Wales (in Sydney, Australia) had developed slowly but steadily during that period and by 1979 we had available all the equipment necessary to revisit the problem of IRUVDR in D_2CO which had been aborted a decade before: a Hänsch-style nitrogen-pumped dye laser system (Molectron UV400/DL200), a home-made pulsed TE CO_2 laser (spark-gap switched, with double-discharge ultraviolet pre-ionization) and a variety of supporting instrumentation. Perhaps the most vital component was a perceptive and persistent

postdoctoral fellow, Dr Gary Nutt, whose efforts finally brought IRUVDR in D_2CO to fruition in July 1979. The first published report of Orr and Nutt (1980a) showed the ability of the 10 P(36) CO_2-laser line to prepare D_2CO molecules in the $v_4=1$, $(J, K_a, K_c)=(8, 1, 7)$ rovibrational state of their ground electronic manifold and the resulting enhancement of the corresponding four rovibronic transitions in the 365 nm 4_1^0 band (two additional transitions being forbidden in this case, owing to the properties of an asymmetric rotor). The quality of the IRUVDR spectrum in this early report was poor by current standards, but it sufficed to provide a convincing demonstration of a genuine state-specific IRUVDR effect and to start to characterize collision-induced rotational relaxation.

Refinements of apparatus, technique, and the scope of results steadily followed the original report of IRUVDR in D_2CO. Orr and Nutt (1980b) introduced a background-subtraction technique to record IRUVDR difference spectra, yielding a much-improved version of the above-mentioned 10 P(36) resonance and its rotational relaxation. The 10 P(16) resonance displayed in figure 2 was also reported, as were a number of IRUVDR results for HDCO. Orr and Haub (1981, 1984) improved the signal-to-noise ratio by using a thyratron to switch the pulsed CO_2 laser. This gave access to some unusual rovibrational excitation effects within the ν_4 vibrational ladder of D_2CO (Orr and Haub 1981) and enabled our first detailed kinetic study of state-to-state rotational energy transfer, initiated by the 10 P(16) CO_2-laser line (Orr *et al.* 1981). Orr and Haub (1984) surveyed the spectroscopic aspects of IRUVDR in D_2CO and HDCO, including several IRUVDR excitation schemes in which a rovibrational transition in the ν_6 band was pumped and the previously unobserved 366 nm 6_1^0 rovibronic band was probed. Digital recording of IRUVDR state-resolved kinetic

Table 1. A selection of IRUVDR excitation schemes involving D_2CO, on which various energy transfer studies have been based. Orr and Haub (1984) give more comprehensive tables.

Infrared transitions		Rovibrational level(s), **1**	IRUVDR $\tilde{A}\leftarrow\tilde{X}$ PROBE, **2**←**1**	References to published results
CO_2 laser	PUMP, **1**←**0**			
10 P(36) 929·017 cm^{-1}	$\nu_4\ {}^{P}Q_2^{(o)}(8)$ 929·030 cm^{-1}	$v_4=1, 8_{1,7}$	$4_1^0\ {}^{r}R, {}^{r}Q, {}^{r}P,$ ${}^{P}Q$	Orr and Nutt (1980a) Orr and Nutt (1980b)
10 P(16) 947·742 cm^{-1}	$\nu_4\ {}^{r}Q_2^{(e)}(12)$ 947·739 cm^{-1}	$v_4=1, 12_{3,10}$	$4_1^0\ {}^{r}R, {}^{r}Q, {}^{r}P,$ ${}^{P}R, {}^{P}Q, {}^{P}P$	Orr and Nutt (1980b) Orr *et al.* (1981)
	$2\nu_4-\nu_4\ {}^{r}P_7^{(o/e)}(10)$	$v_4=2, 9_{8,(2/1)}$	$4_2^1\ {}^{r}R_8(9)$	Haub (1985)
10 P(14) 949·479 cm^{-1}	$2\nu_4-\nu_4\ {}^{r}R_1^{(e)}(5)$	$v_4=2, 6_{2,4}$	$4_2^1\ {}^{r}R-{}^{P}P$	Orr and Haub (1981)
	$2\nu_4-\nu_4\ {}^{r}Q_3^{(e)}(8)$	$v_4=2, 8_{4,5}$	$4_2^1\ {}^{r}R-{}^{P}P$	Orr and Haub (1984)
	$2\nu_4-\nu_4\ {}^{r}Q_3^{(o)}(9)$	$v_4=2, 9_{4,5}$	$4_2^1\ {}^{r}R-{}^{P}P$	
	$\nu_6\ {}^{P}P_2^{(o)}(22)$	$v_6=1, 21_{1,20}$	Uncertain	Orr and Haub (1984)
10 R(28) 980·913 cm^{-1}	$\nu_4\ {}^{r}Q_{10}^{(o/e)}(18)$ 981·4 ± 0·5 cm^{-1}	$v_4=1, 18_{10,(8/9)}$	$4_1^0\ {}^{r}R, {}^{r}Q, {}^{r}P,$ ${}^{P}R, {}^{P}Q, {}^{P}P$	Orr and Haub (1984) Orr *et al.* (1984) Bewick *et al.* (1988)
10 R(32) 983·252 cm^{-1}	$\nu_6\ {}^{r}P_1^{(e)}(8)$ 983·27 cm^{-1}	$v_6=1, 7_{2,6}$	$6_1^0\ {}^{r}R, {}^{r}Q, {}^{r}P,$ ${}^{P}Q, {}^{P}P$	Orr and Haub (1984) Haub and Orr (1984) Bewick *et al.* (1985)
	$\nu_6\ {}^{P}R_5^{(o)}(10)$ 983·25 cm^{-1}	$v_6=1, 11_{4,7}$	$6_1^0\ {}^{r}R, {}^{r}Q, {}^{r}P,$ ${}^{P}R, {}^{P}Q, {}^{P}P,$ ${}^{t}R, {}^{t}Q$	Haub and Orr (1987) Bewick and Orr (1989a) Bewick and Orr (1989b)

curves for D_2CO facilitated extensive studies of rotational energy transfer (Orr *et al.* 1984, Bewick *et al.* 1988) and of fast $\nu_6 \rightarrow \nu_4$ transfer (Haub and Orr 1984, 1987, Bewick and Orr 1989a, b, Bewick 1989), initiated respectively by the 10 R(28) and 10 R(32) CO_2-laser lines. Ironically, our initial detection of IRUVDR signals in D_2CO with the 10 R(28) CO_2-laser line was accidental, in the course of experiments with a poorly adjusted CO_2 laser intended to be operating on the nearby 10 R(32) line. Bewick *et al.* (1985) implemented a home-made narrow-band dye laser, and this has enhanced the spectroscopic resolution in studies of rotational relaxation (Bewick *et al.* 1988) and *J*-resolved $\nu_6 \rightarrow \nu_4$ transfer (Bewick *et al.* 1985, Bewick and Orr,1989b, Bewick 1989) in D_2CO. The D_2CO molecule also figured in the first demonstration of LIF-detected Raman–optical double-resonance spectroscopy (King *et al.* 1983), which has subsequently been developed in studies of glyoxal (Duval *et al.* 1985, 1986) and, very recently, acetylene (Chadwick *et al.* 1989).

Table 1 and figure 5 summarize a selection of the most significant IRUVDR excitation schemes encountered in our investigations of D_2CO. These will be discussed in more detail in section 4.

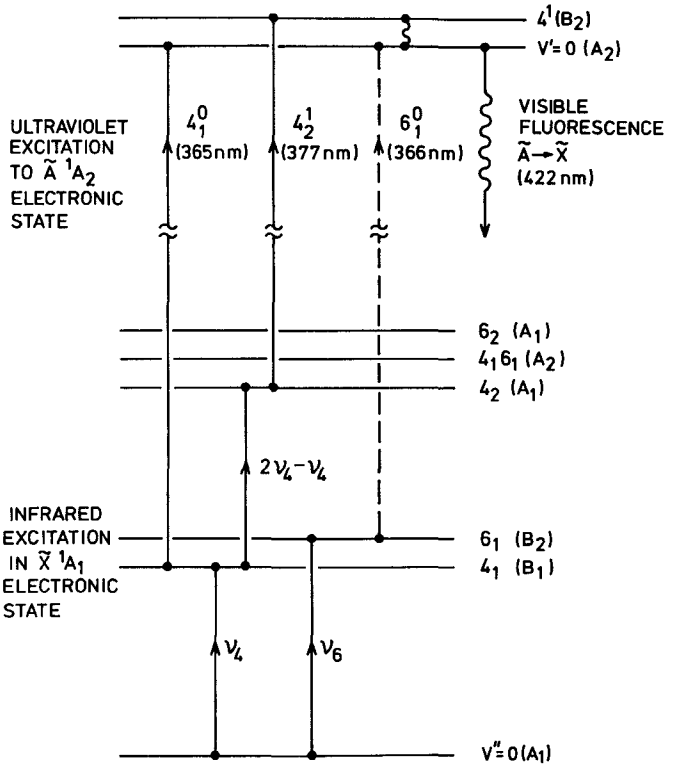

Figure 5. Schemes for infrared-ultraviolet double resonance (IRUVDR) excitation and detection in molecular D_2CO. CO_2-laser excitation proceeds through single rovibrational transitions of the ν_4, ν_6, or $(2\nu_4 - \nu_4)$ bands and is followed by rotationally resolved dye-laser excitation of correlated transitions in the 4_1^0, 6_1^0, and 4_2^1 vibronic bands and visible-fluorescence detection. The 6_1^0-band transition is represented by a broken line, to indicate its low probability. Vibronic symmetry species are indicated in parentheses (Orr and Haub 1984).

4. Spectroscopic subtleties

It is relevant now to explain some of the spectroscopic properties of D_2CO which have enabled our IRUVDR experiments to be contrived. Many aspects of the spectroscopy of formaldehyde have been comprehensively reviewed by Clouthier and Ramsay (1983). At the same time, Moore and Weisshaar (1983) have reviewed the photochemistry and photophysics of formaldehyde.

In its $\tilde{X}^1A_1$ ground electronic state, D_2CO is a planar asymmetric rotor, with its axis of least moment of inertia, labelled *a*, directed along the C=O bond and its *c* axis perpendicular to the molecular plane. Its rotational states are therefore specified by three quantum numbers: J, K_a, K_c; these are often presented in the format, J_{K_a,K_c}. The difference between the rotational constants B and C is small, so that the molecule is a near-prolate rotor. This means that, at sufficiently high values of K_a and/or low values of J, the third quantum number K_c may be suppressed and the molecule may be treated approximately as a prolate symmetric rotor. A similar near-prolate rotor description also applies to the $\tilde{A}^1A_2$ upper electronic state involved in the IRUVDR excitation scheme.

The infrared absorption of D_2CO in the 9–12 μm region (where CO_2 lasers operate) comprises three overlapping fundamental rovibrational bands which correspond to three modes of vibration: ν_3 (CD_2 angle bend, band origin at 1100·4 cm^{-1}, symmetry species a_1), ν_4 (out-of-plane bend, 938·0 cm^{-1}, b_1), and ν_6 (in-plane CD_2 wag, 989·25 cm^{-1}, b_2). The rotational structure of these bands is influenced by mutual Coriolis rotation–vibration interactions, of which the *a* axis coupling between the ν_4 and ν_6 modes is most pronounced (Clouthier and Ramsay 1983). A portion of the infrared absorption spectrum of D_2CO is shown in figure 4, in a region which is dominated by the ν_6 rovibrational band and which is just on the high-frequency side of the ν_4-band centre.

Orr and Haub (1984) have reviewed the wide range of infrared spectroscopic coincidences between CO_2-laser lines and molecular frequencies of D_2CO. These have been established through studies of infrared–radiofrequency double resonance, optically pumped lasers, Lamb-dip absorption, laser-Stark spectroscopy and passive Q-switching, as well as conventional infrared absorption (see figure 4) and IRUVDR spectroscopy itself. Table 1 summarizes some of the most significant of these resonances. The relatively high infrared PUMP pulse intensities employed in our IRUVDR technique tend to produce saturation-broadened linewidths as large as 0·1 cm^{-1}, resulting in a wider range of spectroscopic coincidences between CO_2 laser and molecule than is customary in experiments employing lower-powered c.w. lasers. It should be recognized that our IRUVDR technique does not yield particularly high spectroscopic resolution, owing to our preoccupation with time-resolved studies of molecular energy transfer and the use of pulsed CO_2 and dye lasers which are broader-band than their c.w. counterparts.

The ν_4 mode is of principal interest in the present context, since it is the only mode which can be excited by a CO_2 laser and which shows pronounced Franck–Condon activity in the hot bands of the near-ultraviolet electronic spectrum of D_2CO (Job *et al.* 1969, Strickler and Barnhart 1982); this is consistent with the fact that the molecule is non-rigid and nonplanar in its $\tilde{A}^1A_2$ upper electronic state. Vibronic activity is a necessary aspect of the IRUVDR excitation scheme which has been outlined in figure 1, where the transitions **1**←**0** and **2**←**1** are typically from a fundamental vibrational band and a vibronic hot band respectively, both sharing the same rovibrational level **1**. The most readily accessible excitation scheme in the case of D_2CO therefore comprises an

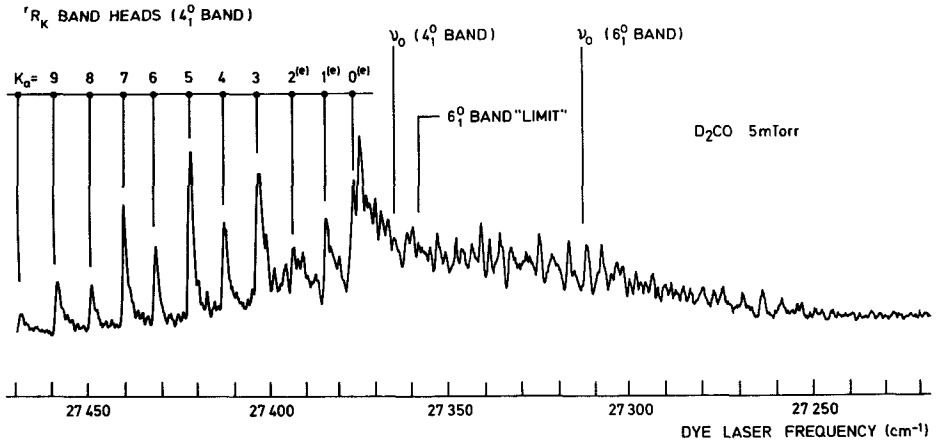

Figure 6. Background LIF excitation spectrum of the 365 nm 4_1^0 and 6_1^0 rovibronic bands of D_2CO, recorded with a sample pressure of 5 mTorr and a dye laser optical bandwidth of $\sim 1\,cm^{-1}$ f.w.h.m.

infrared-pumped transition within the ν_4 band, followed by an ultraviolet-probed transition within a vibronic hot band emanating from the $v_4 = 1$ level of the ground electronic state ($\tilde{X}^1A_1$) of the molecule. The most suitable hot band is the 365 nm 4_1^0 ($v' = 0$, $v_4'' = 1$) band in the vibronically allowed $\tilde{A}^1A_2 \leftarrow \tilde{X}^1A_1$ absorption system of D_2CO, since this is far from the false origin (4_0^1 band, 353 nm) of the system and leaves the molecule in the $v' = 0$ level which has a relatively high fluorescence quantum yield. The 4_1^0 band has been recorded in absorption and over 1000 rovibronic transitions assigned and tabulated (Orr 1974); see also figure 6.

It is also known (Brand 1956, Moore and Weisshaar 1983) that the $\tilde{A} \rightarrow \tilde{X}$ fluorescence spectrum of D_2CO attains maximum intensity near 420 nm where the intense $2_1^0 4_3^0$ and $2_0^0 4_5^0$ vibronic bands coincide, enabling emission from the $v' = 0$ level alone to be monitored with an optical bandpass as broad as 10 nm. Moreover, the fluorescence wavelength (420 nm) is remote from that of excitation (365 nm), which is a consequence of the structural disparity between the ground ($\tilde{X}^1A_1$, rigid planar) and excited ($\tilde{A}^1A_2$, non-rigid, nonplanar) electronic states involved; this enables simple and efficient elimination of scattered laser light. In fact, it was found most appropriate in many of our IRUVDR experiments to use as a broadband filter a piece of acrylic plastic selected to have a suitable absorption edge, blocking 365 nm but transmitting visible light. A further advantage is that the fluorescence quantum yield of D_2CO in the $v' = 0$ or $v_4' = 1$ levels of its $\tilde{A}$ manifold is near unity, substantially greater (and with less rotational-state dependence) than that of H_2CO or HDCO (Moore and Weisshaar 1983).

A further relevant property of D_2CO is the *ortho/para* character of its nuclear-spin modifications, in which the symmetric interchange of two identical nuclei (in this case, the two D nuclei about the molecular *a* axis) causes different quantum states to have different statistical weights (Herzberg 1966, Bunker 1979). In a given vibronic state, rotational states with even and odd values of K_a have statistical weights differing by a factor of two, leading to intensity alternation from one sub-band to the next in any spectrum. For instance, this is evident in the alternating intensities of the ^rR_K sub-band

heads in figure 2(*a*) and again in figure 6. Moreover, once a molecule is prepared in a rovibrational state with a particular value of K_a, collisions tend to preserve the *ortho/para* character so that even-K_a changes take place much more readily than those with odd-numbered changes of K_a.

The above combination of spectroscopic properties provides a sensitive and selective means of monitoring rovibrational excitation involving the ν_4 mode within the electronic ground state, as was first demonstrated by Orr and Nutt (1980a, b) and is exemplified by several of the entries in table 1. The same sensitivity is lacking in the case of the ν_3 and ν_6 modes, since the 3_1^0 and 6_1^0 hot bands of D_2CO have proved too weak to be observed by conventional spectroscopic means. The ν_3 mode is totally symmetric and is therefore unable to contribute to the vibronic transition probability. The ν_6 mode is of b_2 symmetry and is known (Strickler and Barnhart 1982) to contribute marginally to the vibronic intensity of the $\tilde{A}^1A_2 \leftarrow \tilde{X}^1A_1$ system of D_2CO. Orr and Haub (1984) have demonstrated numerous IRUVDR excitation schemes in which a rovibrational transition in the ν_6 band is pumped and the 366 nm 6_1^0 rovibronic band is probed, even though the 6_1^0 band has been estimated (Orr 1974, Orr and Haub 1984) to be 50–200 times less intense than the 4_1^0 band which overlaps it and with which it shares strong *a* axis Coriolis perturbations.

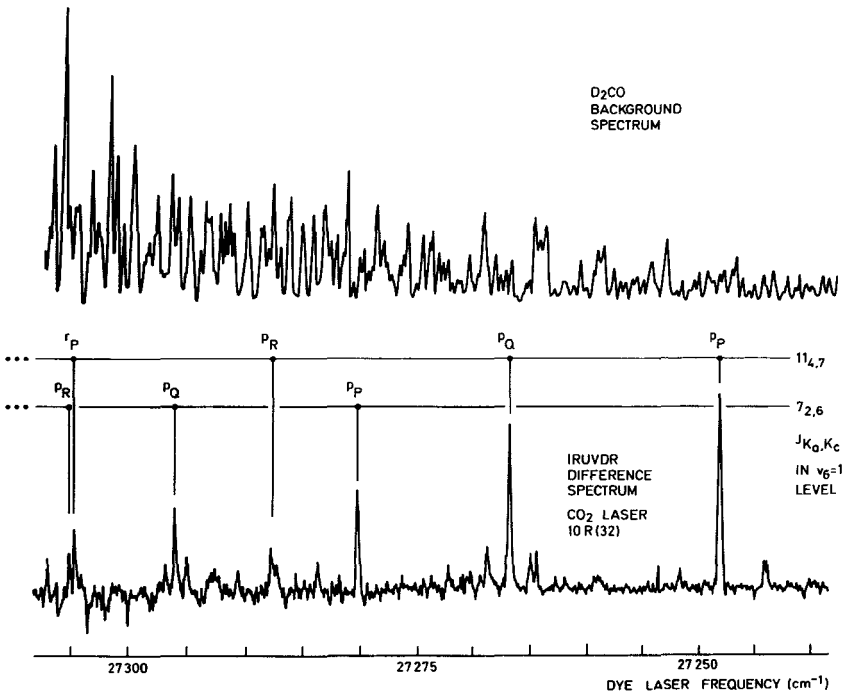

Figure 7. Background LIF excitation spectrum (upper trace) and IRUVDR difference spectrum (lower trace) for the 365 nm 4_1^0 and 6_1^0 vibronic bands of D_2CO. The IRUVDR spectrum was recorded using the 10 R(32) CO_2 laser line and a sample pressure of 50 mTorr with IR–UV delay of 0·1 μs, corresponding to a D_2CO/D_2CO collision number $z = 0{\cdot}05$. The assigned IRUVDR spectral features correspond to excitation of the rovibrational states indicated. Dye laser optical bandwidth is $\sim 0{\cdot}2\,cm^{-1}$ f.w.h.m. (Haub and Orr 1984, 1987, Bewick 1989).

The background LIF excitation spectrum of the $\tilde{A}\leftarrow\tilde{X}$ $4_1^0/6_1^0$ band pair is surveyed in figure 6 (Bewick 1989), with the 4_1^0 and 6_1^0 rovibronic band origins indicated. Also indicated is the high-frequency 'limit' where the ^rR sub-band heads of the 6_1^0 band are expected to bunch together and above which no 6_1^0-band rotational structure is expected, apart from recently identified weak *t*-type ($\Delta K_a = 3$) features (Bewick 1989). The low-frequency end of this LIF excitation spectrum is reproduced with higher resolution in the upper trace of figure 7. Even in this region, the low-frequency tail of the 4_1^0 band is too intense to enable any of the rotational structure of the underlying 6_1^0 band to be identified. The lower trace of figure 7 presents the IRUVDR difference spectrum arising from a $\nu_6/6_1^0$ excitation scheme and recorded under effectively collision-free conditions with a narrow-band ($\sim 0{\cdot}2\ cm^{-1}$) dye laser. Note the markedly superior quality of recent IRUVDR spectra, relative to that of early spectra such as in figure 2(*b*). Selective infrared PUMP excitation by the 10 R(32) CO_2-laser line (see table 1) generates a set of features which can be assigned unambiguously to the 'missing' 6_1^0 band (Orr and Haub 1984, Haub and Orr 1984, 1987). This demonstrates the sensitivity and utility of the IRUVDR technique in exploring weak and/or heavily overlapped molecular rovibronic absorption spectra.

Although this review is concerned primarily with D_2CO, it is instructive to consider briefly the HDCO molecule which, by virtue of its different symmetry, presents several contrasting features in the context of IRUVDR studies (Orr and Haub 1984, Haub and Orr 1987). HDCO lacks the nuclear-spin statistical properties of D_2CO (or H_2CO); this distinction is clearly manifested in collision-induced energy transfer where changes of K_a can be either odd or even (Bewick *et al.* 1988), as well as in different rovibrational and rovibronic intensity distributions. A disadvantage in IRUVDR studies of HDCO is that its fluorescence quantum yield is ~ 20 times less than that of D_2CO, which degrades the detection sensitivity (Orr and Nutt 1980). Nevertheless, a wide range of IRUVDR excitation schemes have been demonstrated in HDCO (Orr and Nutt 1980, Orr and Haub 1984) and these have enabled studies of rotational relaxation (Bewick *et al.* 1988) and V–V transfer (Haub and Orr 1987). In fact, our first experimental evidence that Coriolis coupling could enhance the efficiency of mode-to-mode vibrational energy transfer was obtained in 1981 in the context of HDCO/HDCO collisions, prior to its detailed study in D_2CO/D_2CO collisions as discussed in sections 6 and 7 (Haub and Orr 1984, 1987).

5. *J*-changing rotational energy transfer in D_2CO/D_2CO collisions

Rotational energy transfer (RET) in molecular collisions has been the subject of intensive investigation, both experimental and theoretical, for many years and is now well characterized in most respects (Oka 1973, Brunner and Pritchard 1982, McCaffery *et al.* 1986). However, there is still much to be learned about RET when the colliding molecules are polyatomic with a strongly anisotropic intermolecular potential, as is the case in D_2CO/D_2CO collisions. In this context, the IRUVDR technique has enabled a D_2CO molecule to be prepared by pulsed infrared excitation into a specific rotational state (J_{K_a,K_c}) of the $v_4 = 1$ vibrational level within its $\tilde{X}^1A_1$ ground electronic manifold. This state-selected molecule collides with another collision-partner D_2CO molecule and is transferred to another rotational state ($J'_{K'a,K'c}$) associated with the same vibrational level, the process being monitored by laser-induced fluorescence (LIF). These experiments (Orr *et al.* 1981, 1984, Bewick *et al.* 1988) do not discriminate between the variety of available collision-partner states, but it can be inferred that the vast majority of these belong to the ground vibrational level ($v = 0$) and that RET cross-

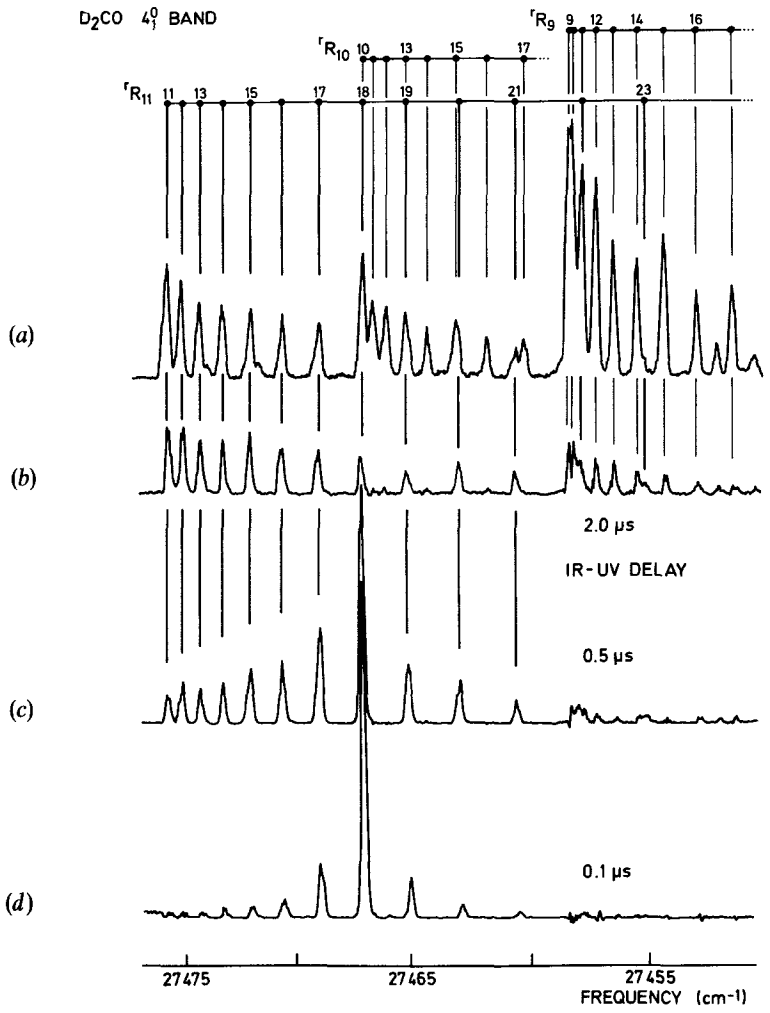

Figure 8. Background (*a*) and IRUVDR difference (*b*), (*c*), (*d*) spectra for D_2CO ($P = 50$ mTorr), recorded with a PROBE dye-laser bandwidth of $\sim 0{\cdot}2\,cm^{-1}$ f.w.h.m. The IRUVDR spectra were obtained with the 10 R(28) CO_2-laser line and IR–UV delays as indicated; the corresponding D_2CO/D_2CO collision numbers z are: (*b*) 1·0, (*c*) 0·25, and (*d*) 0·05. The instrumental gain used in recording trace (*b*) was twice that for traces (*a*), (*c*), and (*d*). The IRUVDR spectra are dominated in this region by RET within the $^rR_{11}$ sub-band of the $\tilde{A} \leftarrow \tilde{X}$ 4_1^0 rovibronic band (Bewick *et al.* 1988).

sections are favoured by changes in rotational quantum numbers which minimize the net rotational energy deficit and thereby minimize the extent to which molecular rovibrational energy needs to be converted into translational energy.

Our most thorough IRUVDR studies of RET (Orr *et al.* 1984, Bewick *et al.* 1988) have concentrated on processes which cause the rotational quantum numbers J and J' for the state-selected D_2CO molecule to differ. These have taken advantage of the rovibrational resonance of D_2CO with the 10 R(28) line of a CO_2 laser (see table 1), yielding kinetic information on RET with relatively large rotational quantum number changes $|\Delta J|$. This is demonstrated qualitatively in figure 8, which shows IRUVDR

difference spectra corresponding to the relaxation of population initially prepared in the $\tilde{X}$, $v_4=1$, $(J, K_a)=(18, 11)$ rovibrational level of D_2CO; as the delay between the IR PUMP and UV PROBE pulses (and hence the D_2CO/D_2CO collision number, z) is increased, collision-induced RET to other J'-levels of the $\tilde{X}$, $v_4=1$, $K_a=11$ manifold is clearly discernible, with $|\Delta J|$ as high as 7. Although such opportunities to observe high-$|\Delta J|$ RET are abundant in the case of diatomic molecules (Brunner and Pritchard 1982, Copeland and Crim 1983, 1984, McCaffery *et al.* 1986), they are rare in the dipolar polyatomic case. This application of IRUVDR has therefore proved useful in testing the appropriateness of different scaling laws and propensity rules potentially able to model RET in dipolar polyatomics.

Figure 9 depicts the IRUVDR sequential excitation scheme relevant to our studies of J-changing rotational relaxation in D_2CO/D_2CO collisions and corresponding to the type of processes already illustrated in figure 8. The infrared PUMP pulse, provided by the 10 R(28) line of a CO_2 laser, prepares a D_2CO molecule in a particular rotational state, $(J, K_a)=(18, 11)$, of the first vibrational level of its ν_4 mode. The tunable ultraviolet PROBE pulse then interrogates the selective rovibrational excitation and its subsequent collision-induced dissipation, using LIF detection. The state preparation by the PUMP can be characterized by recording the 'parent' IRUVDR difference

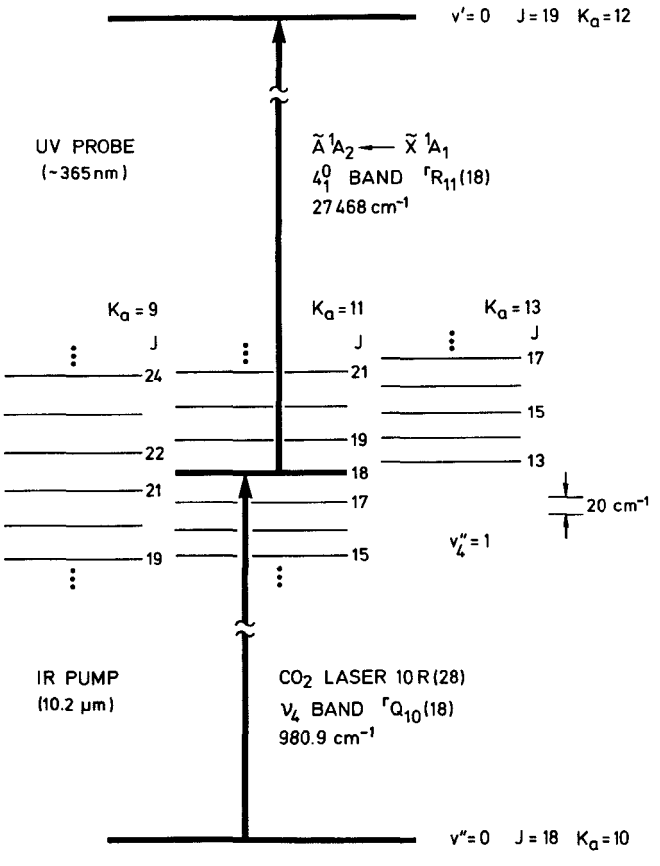

Figure 9. Sequential IRUVDR excitation scheme for D_2CO molecules pumped by the 10 R(28) line of a CO_2 laser (Bewick *et al.* 1988).

spectrum (the difference between LIF excitation spectra with and without infrared PUMP radiation) under conditions of low sample pressure and short IR–UV delay, as in figure 8 (*d*); this corresponds to a small value of the D_2CO/D_2CO collision number z and hence to conditions which allow little or no relaxation of the initially prepared rovibrational population. A rovibronic PROBE transition which is particularly convenient for this purpose is shown explicitly in figure 9: it is the $^rR_{11}(18)$ transition in the 4_1^0 vibronic hot band in the $\tilde{A}^1A_2 \leftarrow \tilde{X}^1A_1$ electronic absorption system of D_2CO. The J-changing RET processes of interest comprise collision-induced RET from the initially prepared $\tilde{X}$, $v_4 = 1$, $(J, K_a) = (18, 11)$ rovibrational level to other levels $(J', 11)$ of the $\tilde{X}$, $v_4 = 1$ manifold. This rotational relaxation can be monitored by recording a set of IRUVDR difference spectra, as in figures 8 (*b*)–(*d*), with successively increasing values of IR–UV delay (and hence collision number z) and watching the growth of 'satellite' features associated with various J'-levels in the $\tilde{X}$, $v_4 = 1$, $K_a = 11$ manifold. Once the overall pattern of RET has been identified in this way, kinetic curves showing the growth and decay of particular IRUVDR features (and hence of particular J'-states) can be generated by scanning the IR–UV delay with PROBE wavelength fixed.

Several spectroscopic aspects of the above excitation scheme make it especially useful for studies of collision-induced RET with relatively large rotational quantum number changes $|\Delta J|$: the fortuitously close coincidence between the $\nu_4\,^rQ_{10}(18)$ rovibrational transition of D_2CO and the 980·913 cm^{-1} 10 R(28) CO_2-laser line (Orr and Haub 1984); the negligibly small asymmetric-rotor splittings in this region of the spectrum, which enable the rotational quantum number K_c to be suppressed in this context; the high value of $K_a = 11$ which prevents the relevant $^rR_{11}$ sub-band of the $\tilde{A} \leftarrow \tilde{X}\, 4_1^0$ vibronic band from forming a sub-band head, as is the case when $J \approx 9$ at lower values of K_a (Orr 1974); the relatively uncongested and compact region of the 4_1^0 rovibronic band in which the $^rR_{11}$ sub-band falls, causing numerous $\tilde{X}$, $v_4 = 1$, $K_a = 11$ rotational states (with J ranging from 11 to 21) to be discernible in IRUVDR difference spectra; the negligible rate of interconversion of *ortho* and *para* nuclear-spin modifications of D_2CO, which ensures that RET is confined to energy levels with odd K_a in the $\tilde{X}$, $v_4 = 1$ manifold on the time scale of these experiments. Most of these aspects are apparent in figure 8.

Useful information in this context is by no means confined to the $4_1^0\,^rR_{11}$ sub-band, for other IRUVDR signals are measurable in the accompanying $^rQ_{11}$, $^rP_{11}$, $^pR_{11}$, $^pQ_{11}$ and $^pP_{11}$ sub-bands. This is illustrated by survey IRUVDR spectra in figure 10, which further demonstrate the effects of collision-induced J-changing RET in D_2CO as well as the extent of K_a-changing RET with $\Delta K_a = -2, -4, -6$, and -8, all of which occur with approximately gas-kinetic collisional efficiencies (Bewick *et al.* 1988). Even at moderate IR–UV delays, this K_a-changing RET tends to obscure the growth and decay of J-changing RET satellites on either side of the prominent $^rQ_{11}(18)$ parent IRUVDR peak. Other observations of K_a-changing RET have been reported by Orr *et al.* (1984).

Figure 11 displays representative kinetic curves measuring the time evolution of IRUVDR intensity in the $^rR_{11}$ sub-band for the parent peak and the $|\Delta J| = 1$ and 2 collision-induced satellites following initial PUMP excitation of the $\tilde{X}$, $v_4 = 1$, $(J, K_a) = (18, 11)$ rovibrational level. The individual points represent the signal-averaged IRUVDR intensity accumulated at each 10 ns interval of the IR–UV delay, covering the range of IR–UV delay t from $-0{\cdot}5$ μs to 4·5 μs. The solid lines represent a triple-exponential least-squares fit to the data, expressed in terms of phenomenological amplitudes and pseudo-first-order rate constants corresponding to a particular D_2CO sample pressure P. These rate constants, which we refer to as *macroscopic*, are

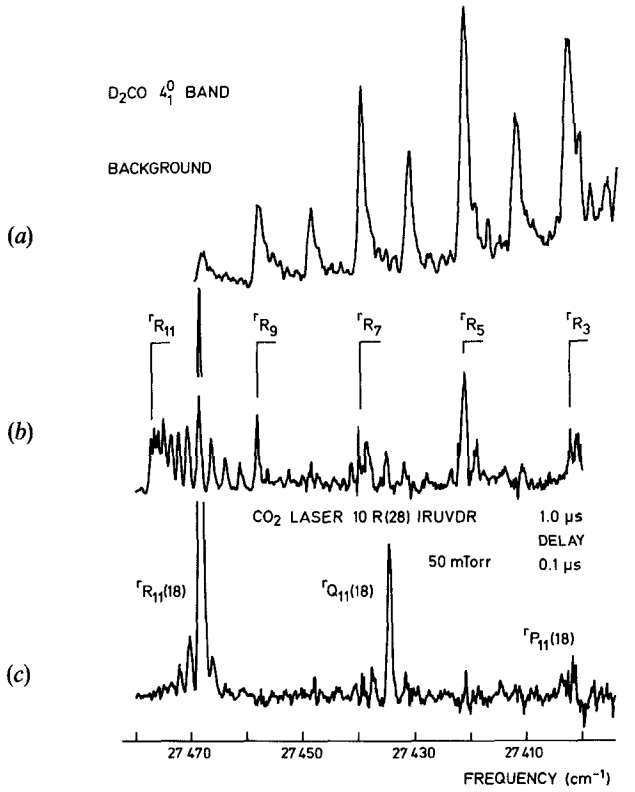

Figure 10. Background (*a*) and IRUVDR difference (*b*), (*c*) spectra, surveying a number of the ^rR and ^rQ sub-bands in the $\tilde{A}\leftarrow\tilde{X}$ 4_1^0 rovibronic band of D_2CO. Trace (*a*) was recorded with $P_{D_2CO}=5$ mTorr. The IRUVDR spectra were obtained with the 10 R(28) CO_2-laser line, $P_{D_2CO}=50$ mTorr, and IR–UV delays as indicated; the corresponding collision numbers z are: (*b*) 0·5 and (*c*) 0·05 (Bewick *et al.* 1988).

indicative of the kinetic eigenvalues arising from the rate equations which govern collision-induced RET. They provide a useful preliminary view of the kinetics. However, they should not be confused with *microscopic* state-to-state rate constants, referring to the individual mechanistic relaxation channels which together constitute the details of a kinetic model. The distinction between these two classes of rate constant is not always clearly drawn in the literature of molecular energy transfer and this tends to confuse comparison between results from different sources.

To understand the kinetics of collision-induced RET in D_2CO and to deduce microscopic rate constants, Bewick *et al.* (1988) have implemented a kinetic master-equation model, following earlier work by Orr *et al.* (1981, 1984). The populations of a set of rovibrational states are represented by a vector $\mathbf{n}(t)$, the time dependence of which is determined by a matrix $\mathbf{\Pi}$ of pseudo-first-order rate constants (dependent on the collision rate, and hence on pressure P). An additional, P-independent matrix $\delta\mathbf{\Pi}(t)$ is used to incorporate the effects of radiative pumping from the ground state to the prepared state; this pumping contribution has a time-dependence which emulates that

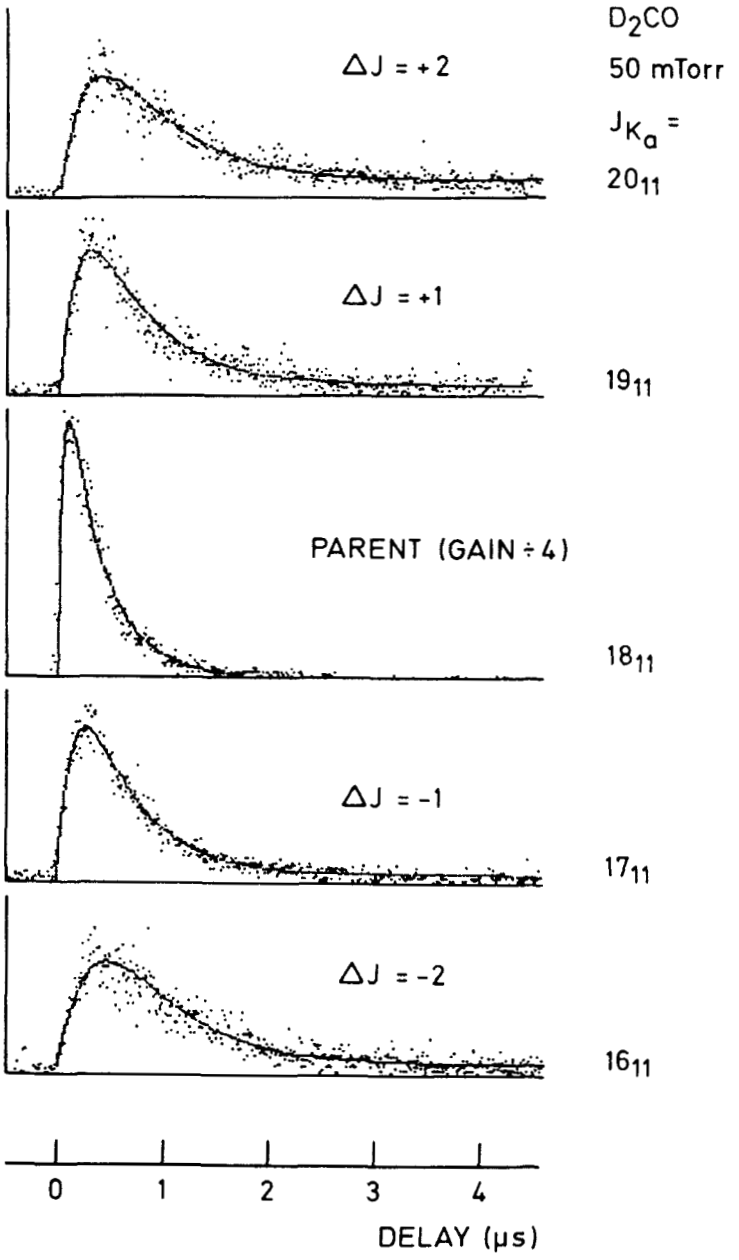

Figure 11. Representative IRUVDR kinetic curves measuring growth and decay of population in the $\tilde{X}$, $v_4 = 1$, $(J, K_a) = (18, 11)$ parent rovibrational level of D_2CO, and in its $\Delta J = \pm 1$ and ± 2 collision-induced satellites. The results were obtained by probing the $^rR_{11}$ subband of the $\tilde{X}\ 4_1^0$ rovibronic band, as portrayed in figure 8; the ordinates are in arbitrary IRUVDR intensity units. The data are for $P_{D_2CO} = 50$ mTorr, so that the IR–UV delay time scale of 0–4·5 μs corresponds to D_2CO/D_2CO collision numbers z ranging from 0 to 2·3. Each plot comprises 512 data points, obtained by averaging over approximately 3000 laser shots, with a triple-exponential curve of best-fit superimposed. The average of several such plots for each rotational state is used in subsequent kinetic modelling (Bewick *et al.* 1988).

of the CO_2-laser PUMP pulse. The set of simultaneous linear rate equations which control rotational relaxation is then expressed in matrix form by

$$\mathbf{dn}(t)/\mathrm{d}t = -[\mathbf{\Pi} + \delta\mathbf{\Pi}(t)] \cdot \mathbf{n}(t). \tag{1}$$

The kinetic matrix $\mathbf{\Pi}$ is constructed to satisfy certain conservation, symmetry and detailed-balance conditions. Consecutive processes due to multiple collisions are included, since non-zero elements of $\mathbf{\Pi}$ are not solely allocated to transitions originating in the directly pumped level.

In order to minimize the number of parameters in the kinetic matrix $\mathbf{\Pi}$, Bewick *et al.* (1988) tested three different fitting laws to represent the functional dependence of the relevant rate constants for $|\Delta K_a| = 0$, J-changing state-to-state RET. Two of these fitting laws depend on scaling with respect to the absolute energy gap $|\Delta E|$ between initial and final states of the state-selected molecule, either as an exponential function of $|\Delta E|$ or as a power law. The third fitting law depends on a propensity rule favouring RET with $|\Delta J| = 1$ and 2. These three fitting laws are known respectively as 'exponential gap' (EG), 'power gap' (PG) and 'propensity rule' (PR) and are chosen to be consistent with fitting laws established in the earlier literature (Oka 1973, Brunner and Pritchard 1982, Copeland and Crim 1983, 1984, McCaffery *et al.* 1986). Additional kinetic terms are included uniformly in each of the models tested to account for loss to molecular levels other than those treated explicitly.

The kinetic master-equation model has been applied successfully by Bewick *et al.* (1988) to J-changing RET within the $\tilde{X}^1A_1$, $v_4 = 1$, $K_a = 11$ rovibrational manifold of D_2CO, as represented by figures 8–11. Kinetic curves predicting the time-development of IRUVDR intensity have been computed as a function of the two adjustable parameters for each of the proposed fitting laws. The computed kinetic curves have then been compared with experimental RET kinetic data, corresponding to the range $J' = 13$–21 within the $K_a = 11$ manifold. A sample of such comparisons, for $\Delta J = 0$ and ± 1, are shown in figure 12. A comparable level of agreement is obtained at higher values of $|\Delta J|$ with both EG and PG models (with the latter marginally superior), but the corresponding comparisons for $|\Delta J| > 2$ become increasingly less adequate in the case of any version of the PR model. We therefore conclude that, in the context of J-changing RET in D_2CO/D_2CO collisions, the EG and PG energy-gap fitting laws are substantially superior to any propensity-rule model which allows direct transfer only with $|\Delta J| = 1$ or 2. The kinetics of RET with ΔJ ranging from $+3$ to -7 cannot be attributed exclusively to consecutive collision-induced processes with individual changes $|\Delta J|$ confined to values of 1 or 2, as specified by the PR fitting law. We infer that the adequacy of propensity rules in earlier descriptions of RET in dipolar polyatomic molecules (Oka 1967, 1973) arises primarily from the limited range of $|\Delta J|$ monitored in such experiments, rather than from any discrepancy with the dipolar diatomic case where energy-gap scaling laws are well established (Brunner and Pritchard 1982, Copeland and Crim 1983, 1984, McCaffery *et al.* 1986). The microscopic state-to-state rate constants for J-changing RET in the D_2CO/D_2CO collisions studied display an approximate factor-of-three decline for each increment of $|\Delta J|$. This reflects the dominance of $\Delta J = \pm 1$ contributions, owing to long-range dipole–dipole interactions. The results obtained in this context by Bewick *et al.* (1988) are remarkably detailed by standards normally applied to RET in dipolar polyatomic molecules, particularly with regard to the range of $|\Delta J|$ monitored and the corresponding quality of the fitting laws derived. They elucidate RET in collisions between a pair of dipolar polyatomic (D_2CO) molecules at a level of detail usually confined to studies of dipolar diatomic molecules.

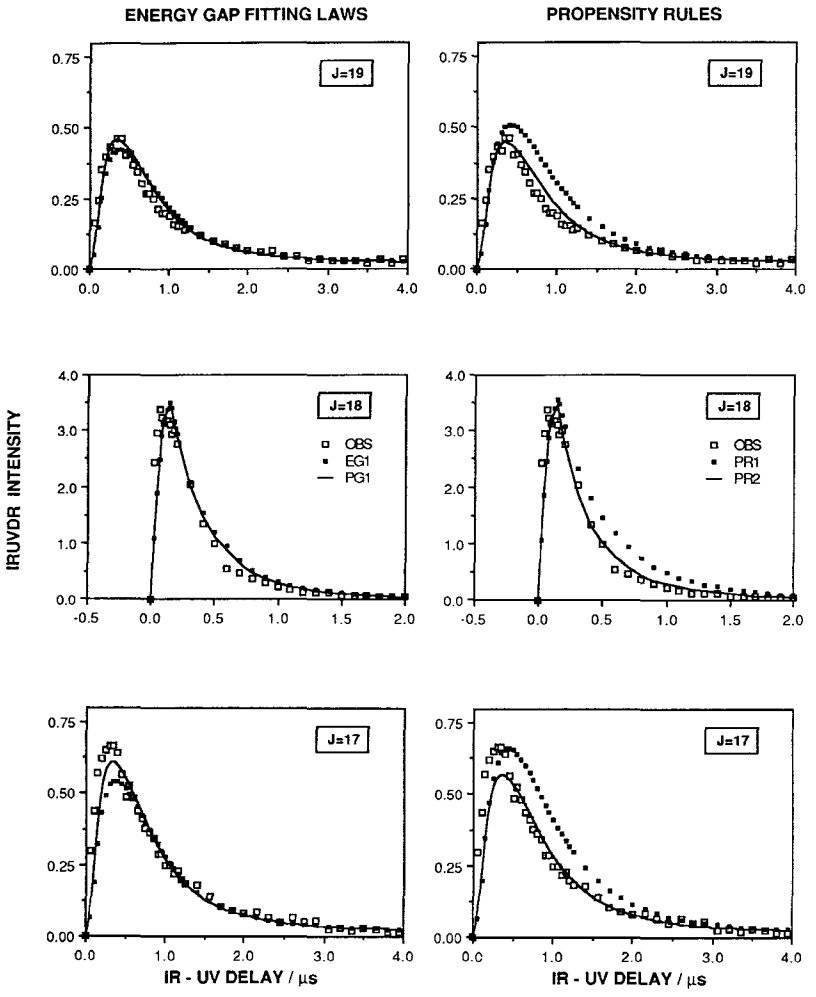

Figure 12. Observed and computed IRUVDR kinetic curves for the $\tilde{X}$, $v_4 = 1$, $(J, K_a) = (18, 11)$ parent rovibrational level and its $\Delta J = \pm 1$ collision-induced satellites. The experimental data points (open symbols) were obtained by probing the $^rR_{11}$ sub-band of the $\tilde{A} \leftarrow \tilde{X}$ 4_1^0 rovibronic band of D_2CO with $P_{D_2CO} = 50$ mTorr, as in figure 10. The left-hand set of plots shows the results of kinetic modelling of RET based on two energy-gap fitting laws: EG1 (exponential gap, black symbols) and PG1 (power gap, line plots). The right-had set illustrates two different forms of propensity-rule (PR1 and PR2) modelling. Note that plots for the $J = 18$ parent have a different ordinate and abscissa to those for the $\Delta J = \pm 1$ satellites (Bewick *et al.* 1988).

6. Efficiency of collision-induced V–V transfer in D_2CO

One of the most powerful applications of the IRUVDR technique has been in characterizing an unusually efficient class of collision-induced mode-to-mode vibrational energy transfer process occurring in D_2CO and HDCO. The high efficiency of such processes arises from a subtle combination of Coriolis coupling (i.e. rovibrational mixing) and asymmetric-rotor perturbations, as will be demonstrated here in the case of $\nu_6 \rightarrow \nu_4$ transfer in D_2CO (Haub and Orr 1984, 1987, Bewick *et al.* 1985, Bewick and Orr 1989a, b).

The variation of IRUVDR technique employed here has the excitation scheme depicted in figure 13 and enables detailed characterization of processes of the following type:

$$D_2CO(v_6=1; J, K_a, K_c) + M \rightarrow D_2CO(v_4=1; J', K_a', K_c') + M. \quad (2)$$

Here a D_2CO molecule is prepared by pulsed infrared excitation into a specific rotational state (J, K_a, K_c) of the first vibrational level of its ν_6 mode. This selective rovibrational excitation can be characterized by recording the parent IRUVDR difference spectrum under conditions of low sample pressure and short IR–UV delay, corresponding to a small value of the D_2CO/D_2CO collision number z and hence to conditions which allow little or no relaxation of the initially prepared rovibrational population. As before, the processes of interest are monitored by vibronic LIF.

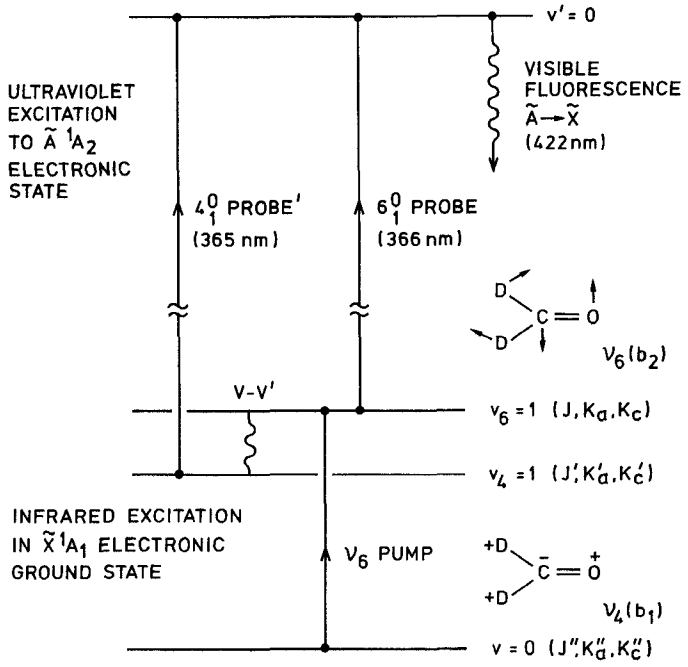

Figure 13. General excitation scheme for time-resolved IRUVDR studies of collision-induced $\nu_6 \rightarrow \nu_4$ rovibrational energy transfer in D_2CO vapour. A CO_2-laser PUMP pulse selects a single rovibrational state $v_6 = 1$ (J, K_a, K_c). The population changes created by the PUMP radiation are then monitored by vibronically excited LIF, either directly in the 366 nm 6_1^0 hot band (PROBE) or indirectly, after $\nu_6 \rightarrow \nu_4$ transfer to the state $v_4 = 1$ (J', K_a', K_c'), in the 365 nm 4_1^0 hot band (PROBE') (Haub and Orr 1987).

Collisions between the state-selected D_2CO molecule and a collision partner M (which may in general be atomic or molecular, but which is confined to D_2CO itself in this section) induce V–V transfer from the initially prepared ν_6-mode state to particular rotational states (J', K'_a, K'_c) of the first vibrational level of the adjacent ν_4 mode of D_2CO. This V–V transfer is studied by recording a set of IRUVDR spectra with successively increasing values of IR–UV delay (and hence collision number z) and watching the growth of spectral features associated with the ν_4 mode. This is illustrated in figure 14, in the case of D_2CO molecules excited by the 10 R(32) CO_2-laser line. A portion of the corresponding parent IRUVDR spectrum has already been presented in figure 7. Once the favoured rovibrational channels of V–V transfer have been identified as in figure 14, kinetic curves showing the growth and decay of particular IRUVDR features at a given pressure are generated by varying the delay with PROBE wavelength fixed, as shown in figure 15. The solid curves in figure 15 derive from detailed kinetic modelling, to be described in section 7 (Bewick and Orr 1989a). The significantly faster growth rate of the $K_a = 6$ signals is consistent with a mechanism in which the dominant channel of $\nu_6 \rightarrow \nu_4$ transfer is that with $K_a = 4 \rightarrow 6$ (Haub and Orr 1984, 1987).

The above experimental strategy is enhanced by several spectroscopic subtleties. Within the $\tilde{A}^1A_2 \leftarrow \tilde{X}^1A_1$ electronic absorption system of D_2CO, the 6_1^0 and 4_1^0 vibronic hot-band transitions are appropriate to monitor rovibrational populations associated respectively with the $v_6 = 1$ and $v_4 = 1$ vibrational levels. As mentioned in section 4, the 4_1^0 band is relatively strong and well characterized (Orr 1974), but the adjacent 6_1^0 band is extremely weak and heavily overlapped by the 4_1^0 band (see figures 6 and 7). In monitoring V–V transfer with high sensitivity, the strong 4_1^0 band is preferred to the weak 6_1^0 band (which is then only required to characterize the rovibrational states prepared by the PUMP laser, as in figure 7); it is therefore advantageous to study $\nu_6 \rightarrow \nu_4$ transfer in D_2CO, rather than the reverse $\nu_4 \rightarrow \nu_6$ transfer process. It is also advantageous to monitor $v_4 = 1$ rovibrational population through the well defined ^rR sub-bands at the high-frequency end of the 4_1^0 band, well above the 6_1^0 band 'limit' where r- and p-type ($\Delta K_a = \pm 1$) parent sub-bands cannot interfere with spectral features attributable to $\nu_6 \rightarrow \nu_4$ transfer.

In the case of self-collisions (M = D_2CO), Haub and Orr (1984, 1987) have found the macroscopic collisional efficiency for $\nu_6 \rightarrow \nu_4$ transfer to be greater than gas-kinetic, indicating that V–V transfer can take place at longer range than that of hard-sphere collisions. This efficiency is remarkably high, for typical V–V energy transfer efficiencies usually lie in the range 10^{-1} to 10^{-4} per hard-sphere collision. Even vibrational 'ladder-climbing' processes, involving collision-induced relaxation within the manifold of vibrational levels associated with a single mode, are usually expected to occur at rates which are much slower than gas-kinetic (Yardley 1980, Weitz and Flynn 1981, Orr and Smith 1987). The extraordinarily high efficiency of mode-to-mode transfer arising in D_2CO/D_2CO collisions has been rationalized by Haub and Orr (1984, 1987) in terms of a semiclassical collision theory, based on long-range electric dipole–dipole interactions. The essential mechanism depends on the strong Coriolis interaction between the ν_4 and ν_6 vibrational modes of D_2CO, which mixes rotation-vibration basis states and yields non-vanishing matrix elements of the *permanent* electric dipole moment μ between the ν_4 and ν_6 vibrational manifolds. Whereas conventional long-range theories of V–V transfer depend on interactions between *oscillating* electric dipoles (in addition to contributions from the short-range part of the intermolecular potential), it now becomes appropriate to use a collision theory of the form normally

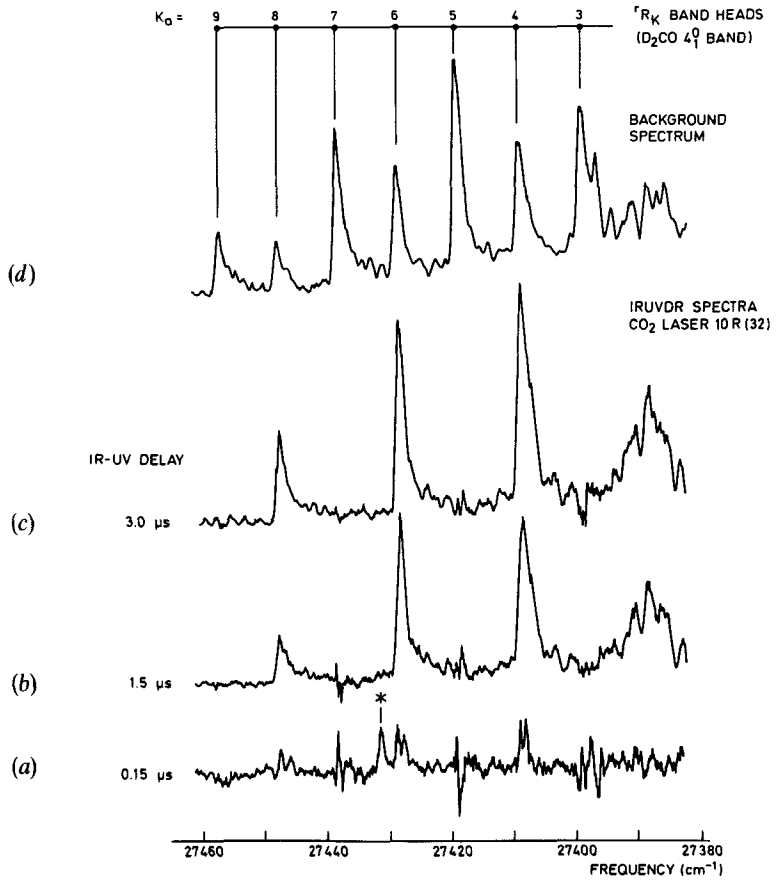

Figure 14. Collision-induced growth of IRUVDR intensity on the short-wavelength side of the 365 nm 4_1^0 band of D_2CO, obtained with the 10 R(32) CO_2-laser line and $P_{D_2CO} = 50$ mTorr. Traces (*a*)–(*c*) are IRUVDR difference spectra recorded with the following values of D_2CO/D_2CO collision number z: 0·075, 0·75, 1·5, respectively. Trace (*a*) is effectively a null trace, apart from subtraction noise and the IRUVDR feature marked with an asterisk, which has recently been assigned to the weak $^tR_4(11)$ parent peak of the 6_1^0 band. Trace (*d*) is the corresponding background LIF excitation spectrum (comparable to the high-frequency end of figure 6). Under the conditions of traces (*b*) and (*c*), considerable IRUVDR intensity appears; this is attributed to collision-induced V–V transfer between the ν_6 and ν_4 vibrational modes. All spectra are recorded with a PROBE dye-laser bandwidths of $\sim 0{\cdot}7\,cm^{-1}$ f.w.h.m. (Haub and Orr 1984, 1987, Bewick 1989).

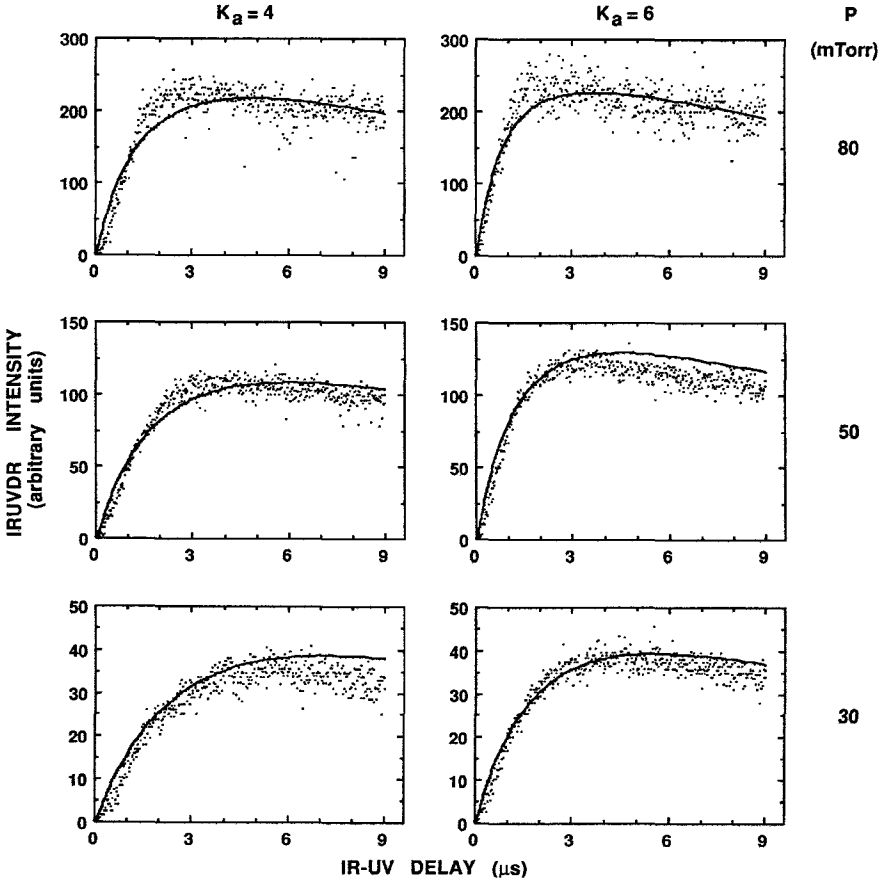

Figure 15. Kinetic curves demonstrating the growth and initial decay of the intensity $I(t)$ of IRUVDR spectral features which correspond to rovibrational states of D_2CO with $v_4 = 1$, $J' \approx 6$–11 and $K'_a = 6$ or $K'_a = 4$. The digitally recorded kinetic curves are the result of 10 R(32) CO_2-laser excitation of states in the $v_6 = 1$ level of D_2CO, with subsequent $v_6 \rightarrow v_4$ transfer. The abscissa of each plot is the IR–UV delay t, between ultraviolet PROBE and infrared PUMP laser pulses. The solid curves are computed in terms of the detailed kinetic model described in section 7. The curves for $P = 50$ mTorr have been computed to fit the experimental results, but those for $P = 30$ and 80 mTorr have been obtained without any further adjustment of second-order rate constants or other kinetic parameters, apart from scaling of the overall amplitudes at each volume of P. The plots within each row cover a range of D_2CO pressures P (Bewick and Orr 1989a).

applied to pure rotational relaxation, rather than to conventional V–V transfer. In fact, the simplest interpretation of (2) would be to suppose that the initial and final eigenstates of the state-selected D_2CO molecule belong to a single 'grand' (ν_4, ν_6) manifold of rotational states, within which collision-induced transfer can occur at the fast rates characteristic of rotational relaxation. However, such a simple interpretation neglects the inevitable occurrence of destructive quantum-mechanical interferences (Orr and Smith, 1987) and fails to account adequately for the collision-induced rovibrational propensity rules which are observed.

The theoretical treatment of Haub and Orr (1987) evaluates the collisional efficiency relatively crudely in terms of the first-order Born approximation. It is found that a combination of Coriolis and asymmetric-rotor perturbations generates non-zero matrix elements of the permanent electric dipole moment μ between different rovibrational eigenstates of the state-selected molecule; herein lies the major distinction between the present rovibrational energy transfer theory and earlier theories. Another significant feature of the fast V–V transfer which we consider is its apparent quasi-elasticity with respect to the state-selected molecule, such that its internal energy change is very much less than kT. There then exist many initial collision-partner states for which a correspondingly small energy change is probable, yielding an approximately zero overall energy deficit. This contributes to large V–V transfer probabilities by providing 'rotational compensation' of rovibrational energy deficits which might otherwise be relatively large on the basis of vibrational energy alone.

Such behaviour is well illustrated by the efficient V–V transfer channel shown by Haub and Orr (1984, 1987) to exist between the $(v_6=1;11,4,7)$ and $(v_4=1;11,6,6)$ rovibrational eigenstates of D_2CO, activated by 10 R(32) CO_2-laser excitation. The collision-induced transition between these two eigenstates is quasi-elastic, with the energy change of the state-selected molecule as small as $3{\cdot}5\,\mathrm{cm}^{-1}$. The corresponding rovibrational eigenstates can be expressed precisely in terms of products of vibrational basis functions, $|\nu_4\rangle$ and $|\nu_6\rangle$, and symmetric-rotor basis functions, $|J,K\rangle$. Explicit evaluation of the Coriolis-induced electric dipole transition moment then yields:

$$\begin{aligned}&\langle v_6=1;11,4,7|\boldsymbol{\mu}|v_4=1;11,6,6\rangle\\&\quad=\mu(v=0)[0{\cdot}185\langle 11,6|\boldsymbol{\Phi}|11,6\rangle-0{\cdot}187\langle 11,4|\boldsymbol{\Phi}|11,4\rangle+\ldots]\\&\quad=0{\cdot}093\mu(v=0)\langle 11,4|\boldsymbol{\Phi}|11,4\rangle,\end{aligned}\tag{3}$$

where $\boldsymbol{\Phi}$ is the direction cosine between the intra- and intermolecular axes to which the dipole–dipole interactions of the state-selected molecule is referred, and $\mu(v=0)$ is the 'permanent' electric dipole moment (2·35 debye) of the molecule. The 'off-diagonal' nature of (3) with respect to $K_a(=4)$ and $K'_a(=6)$ is vital in ensuring that the transition moment in this case avoids the type of destructive interference mentioned above and discussed at length by Orr and Smith (1987). Such interferences are frustrated in the derivation of (3) by the K-dependence of the symmetric-rotor matrix elements $\langle J',K'|\boldsymbol{\Phi}|J,K\rangle$. Coriolis mixing cannot by itself generate this off-diagonal character, for the a axis Coriolis perturbations which cause the vibrational basis states $|\nu_4\rangle$ and $|\nu_6\rangle$ to be mixed respectively into the $v_6=1$ and $v_4=1$ rovibrational eigenfunctions are unable to mix different basis states $|J,K\rangle$. It is the asymmetric-rotor character of the molecule which introduces a variety of rotational basis functions, with K (or K') different from the value of K_a (or K'_a) used to label the initial (or final) rovibrational eigenfunction, and hence yields a relatively large transition moment between $K_a=4$ and $K'_a=6$ states. We therefore conclude from (3) and its derivation that mixing of

vibration-rotation basis functions, by a combination of Coriolis and asymmetric-rotor perturbations, causes D_2CO to acquire a rovibrational transition moment which corresponds to almost 10% of the permanent electric dipole moment in the ground vibrational level ($v=0$). On this basis, our most recently reported theoretical estimates of the efficiency of the $K_a=4\rightarrow6$ channel of $\nu_6\rightarrow\nu_4$ transfer in D_2CO/D_2CO collisions fall in the range 0·35–1·8 (Bewick and Orr 1989a). Early experimental estimates of this efficiency, based on a macroscopic kinetic analysis, were relatively high at 3·8 (Haub and Orr 1984, 1987). However, detailed kinetic modelling by Bewick and Orr (1989a) now yields an experimentally derived microscopic efficiency of 0·25 or less (see section 7).

The above mechanism has been confirmed by several additional examples (involving either D_2CO/D_2CO or HDCO/HDCO collisions) in which the contributing factors are less favourable and the observed V–V transfer rates are correspondingly smaller (Haub and Orr 1987). It is concluded that only a limited range of initially prepared rovibrational states of D_2CO (or HDCO) fulfil all the pre-requisites needed to achieve direct V–V transfer with high collisional efficiency. These pre-requisites comprise: (*a*) Coriolis coupling between the initial and final rovibrational eigenstates of the state-selected molecule, which enables use of the types of inelastic collision theory normally applicable to pure rotational relaxation; (*b*) a close coincidence in energy between those initial and final eigenstates, thereby enhancing the abundance of collision partners available to yield a zero overall energy defect for the pair of colliding molecules; (*c*) the presence of a secondary intramolecular perturbation (here due to the asymmetric-rotor character of the molecule) capable of frustrating quantum-mechanical cancellations which otherwise tend to annihilate Coriolis-induced transition moments. The combined effect of (*a*) and (*c*) may at first seem surprising, for it means that Coriolis-induced transition moments are most pronounced at moderate values of the rotational quantum number K_a (~4), where both asymmetry and Coriolis perturbations are simultaneously appreciable, rather than at higher values of K_a where Coriolis coupling is itself greatest; this is borne out in the experimental results of Haub and Orr (1987).

Two other theoretical approaches have been taken to explain the mechanism and efficiency of collision-induced $\nu_6\rightarrow\nu_4$ transfer in D_2CO. In a series of recent papers, Parson (1988, 1989, 1990) has provided a useful perspective, showing that there is a direct classical anologue to the above quantum-mechanical mechanism and its subtle interplay of Coriolis and asymmetric-rotor perturbations. The approximate coupled-channel theory of Peet and Clary (1986) has treated the vibrational and K_a-rotational degrees of freedom as quantized, with a classical approximation for the J-rotational motion; their results clearly demonstrate Coriolis enhancement of the $\nu_6\rightarrow\nu_4$ transfer rate for D_2CO/Ar and D_2CO/He collisions, as well as the need to take asymmetric-rotor effects into account. Significant contributions from Coriolis and asymmetric-rotor sources are therefore expected to be intrinsic to any theory—whether long-range or short-range, quantum-mechanical or semi-classical—able to explain fast collision-induced $\nu_6\rightarrow\nu_4$ transfer in D_2CO.

7. Rotationally specific V–V transfer in D_2CO: can molecules remember?

As a general rule, the rate of collision-induced V–V transfer between the vibrational modes of a polyatomic molecule is much less efficient than the rate of rotational relaxation which invariably accompanies V–V transfer. Even in 'fast' vibrational ladder-climbing processes (Weitz and Flynn 1981), rotational relaxation occurs on a

time scale at least an order of magnitude faster than that of V–V transfer. This causes rotational 'scrambling' which tends to obscure rotationally specific channels of V–V transfer, from one rovibrational state to another, and to frustrate attempts to determine experimentally whether some of these channels are markedly more efficient than others. Nevertheless, it is anticipated on theoretical grounds that particular V–V channels, corresponding to certain combinations of initial and final rovibrational state, are indeed favoured in molecular collisions. This situation leads us to seek an answer to the following important fundamental questions: is it possible for a molecule to 'remember' its initial rotational state after undergoing collision-induced vibrational energy transfer, and can rotationally specific channels of V–V transfer be observed? Put another way: can we perform experiments with sufficient state-specificity, sensitivity and time-resolution to be able to discern the favoured rotational destination states to which molecules are transferred in the course of mode-to-mode vibrational relaxation?

An affirmative answer to these questions can be made in the special case of $\nu_6 \rightarrow \nu_4$ transfer in D_2CO, as will be shown in this section. Indeed, section 6 has already demonstrated the predominance of the $K_a = 4 \rightarrow 6$ channel of $\nu_6 \rightarrow \nu_4$ transfer, on both

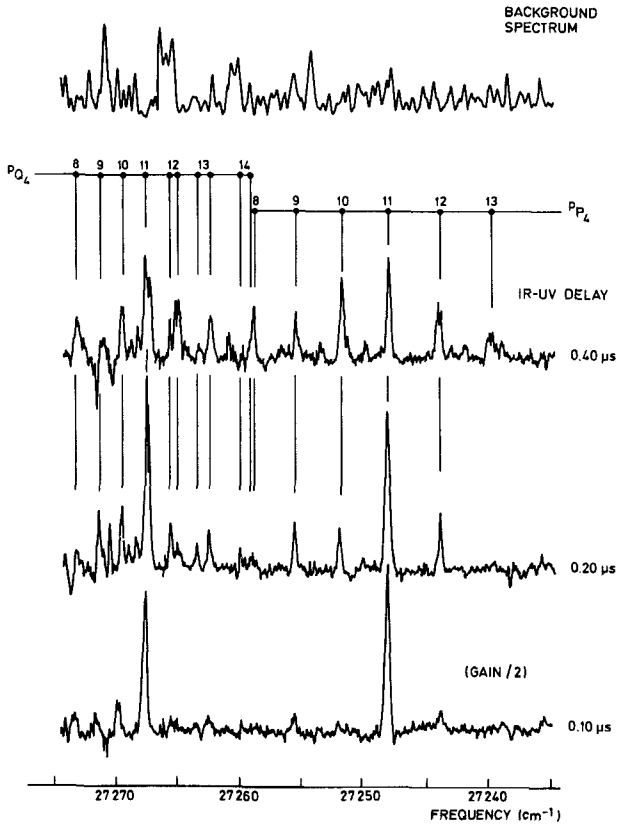

Figure 16. IRUVDR difference (*a*), (*b*), (*c*) and background (*d*) spectra for D_2CO ($P = 50$ mTorr), recorded with a PROBE dye-laser bandwidth of $\sim 0{\cdot}2\,cm^{-1}$ f.w.h.m. The IRUVDR spectra were obtained as in figure 7 with the 10 R(32) CO_2-laser line and the following D_2CO/D_2CO collision numbers z: (*a*) 0·05, (*b*) 0·10, and (*c*) 0·20. The figure shows rotational relaxation in the low-frequency end of the heavily overlapped $\tilde{A} \leftarrow \tilde{X}\ 6_1^0$ vibronic band of D_2CO (Bewick 1989).

theoretical and experimental grounds, and this is itself an example of rotational specificity with respect to the quantum number K_a. There is also evidence of less trivial rotational specificity with respect to the quantum number J, as well as K_a. This evidence derives from J-resolved IRUVDR experiments on collision-induced $\nu_6 \rightarrow \nu_4$ transfer in D_2CO, first performed by Bewick *et al.* (1985), and from detailed kinetic modelling (Bewick and Orr 1989a, Bewick 1989, C. P. Bewick, J. G. Haub, J. F. Martins and B. J. Orr 1989, unpublished results).

J-resolved IRUVDR experiments on $\nu_6 \rightarrow \nu_4$ transfer are more demanding than those which produced results such as those in figure 14, with respect to both signal-to-noise ratio and spectroscopic resolution. The necessary instrumental enhancement, first reported by Bewick *et al.* (1985), has also yielded IRUVDR spectra such as those already presented in figures 7 and 8. In fact, figure 7 is part of the 6_1^0-band parent IRUVDR spectrum for the excitation scheme of interest here; the 10 R(32) CO_2-laser PUMP is seen to prepare D_2CO molecules in the $(J, K_a, K_c) = (7, 2, 6)$ and $(11, 4, 7)$ rotational states of the $v_6 = 1$ vibrational level. The effect of collisions on a portion of that parent IRUVDR spectrum is displayed in figure 16. This is a source of information on the kinetics of J-changing RET in the $v_6 = 1$ rovibrational manifold, accompanying $\nu_6 \rightarrow \nu_4$ transfer (Bewick 1989): this causes the collision-induced growth of satellite features, similar to those studied in greater detail (and with superior sensitivity) in section 5. The IRUVDR spectra needed to demonstrate $\nu_6 \rightarrow \nu_4$ transfer are similar to those in figure 14, but with enhanced PROBE dye-laser bandwidth to resolve individual rotational J-states. Two such sets of spectra are shown in figures 17 and 18 (Bewick 1989). These have been recorded in the vicinities of the $K'_a = 6$ and $K'_a = 4$ ^rR sub-bands in the 4_1^0-band respectively, so that they indicate evolution of population in various J-states in the $K'_a = 6$ and $K'_a = 4$ stacks of the $v_4 = 1$ manifold. The $^rQ_8$ and $^rQ_6$ sub-bands which also appear in figures 17 and 18 give additional information about J-states with $K'_a = 8$ and $K'_a = 6$ respectively.

Figures 17 (*a*) and 18 (*a*) represent effectively collision-free conditions ($z = 0{\cdot}05$). There are discernible IRUVDR features at 27 433 cm^{-1} and 27 411·5 cm^{-1} (asterisked), which are assigned respectively to the $^tR_4(11)$ and $^tQ_4(11)$ transitions (both weakly allowed, with $\Delta K_a = 3$) of the directly excited 6_1^0-band of D_2CO. The former feature (in figure 17 (*a*)) corresponds to the asterisked feature in figure 14 (*a*), which resolves a long-standing puzzle (Orr and Haub 1984, Haub and Orr 1984, 1987) and removes the last vestige of doubt that the strong IRUVDR feature at the high-frequency end of the $4_1^0/6_1^0$ vibronic band region might arise from a source other than the $\nu_6 \rightarrow \nu_4$ transfer process of interest. These $^tR_4(11)$ and $^tQ_4(11)$ feature provide a convenient indication of the parent state population in spectral regions that also display the growth of $v_4 = 1$ rovibrational population due to $\nu_6 \rightarrow \nu_4$ transfer. There is some initial growth of IRUVDR signal in the vicinity of the 4_1^0 $^rR_6$ sub-band head ($\sim 27\,430\ cm^{-1}$ in figure 17 (*a*)), which Bewick *et al.* (1985) attributed to the onset of a dominant J-selective $K_a = 4 \rightarrow 6$ channel of $\nu_6 \rightarrow \nu_4$ transfer. The corresponding region near the 4_1^0 $^rR_4$ sub-band head ($\sim 27\,410\ cm^{-1}$ in figure 18 (*a*)) yields an effectively null signal, which is consistent with that proposition.

The effect of D_2CO self-collisions is illustrated in figures 17 (*b*)–(*d*) and 18 (*b*)–(*c*). Collisions cause the $^tR_4(11)$ and $^tQ_4(11)$ parent features to decay markedly as adjacent RET satellite structure grows, owing to rotational relaxation in the manner of figure 16. The more prominent features, which grow as collision number z increases, indicate the combined effects of $\nu_6 \rightarrow \nu_4$ transfer and RET (both J- and K_a-changing), which tend to occur simultaneously. The 'amplification factor' derived from the large transition

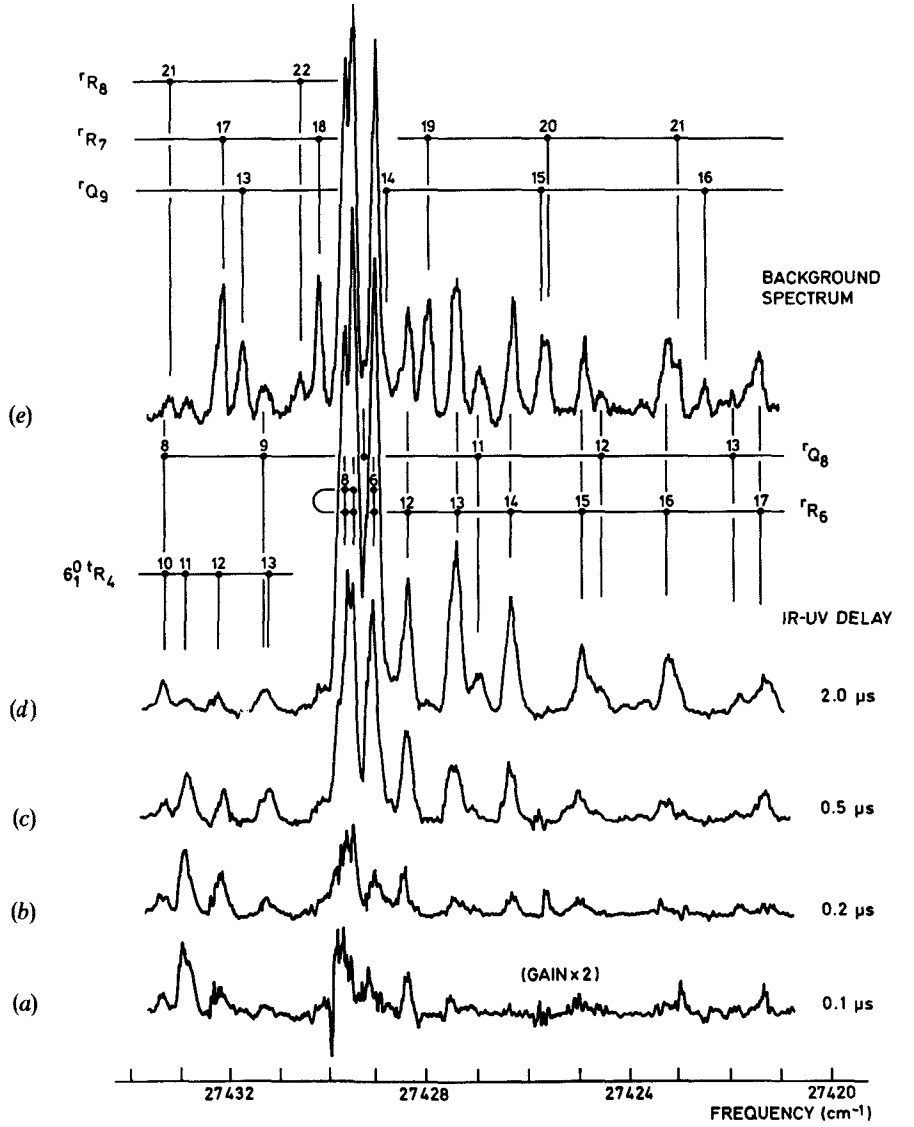

Figure 17. *J*-resolved collision-induced growth of IRUVDR intensity in the vicinity of the $^rR_6$ sub-band of the $\tilde{A}\leftarrow\tilde{X}$ 4_1^0 vibronic band of D_2CO, recorded with a PROBE bandwidth of $\sim 0{\cdot}2\,cm^{-1}$ f.w.h.m. Note the weak $^tR_4(11)$ parent peak of the 6_1^0 band. Traces (*a*)–(*d*) are IRUVDR difference spectra recorded with $P_{D_2CO} = 50$ mTorr and D_2CO/D_2CO collision number $z = 0{\cdot}05$, $0{\cdot}10$, $0{\cdot}25$ and $1{\cdot}0$ respectively. Trace (*e*) is a background LIF excitation spectrum (Bewick 1989).

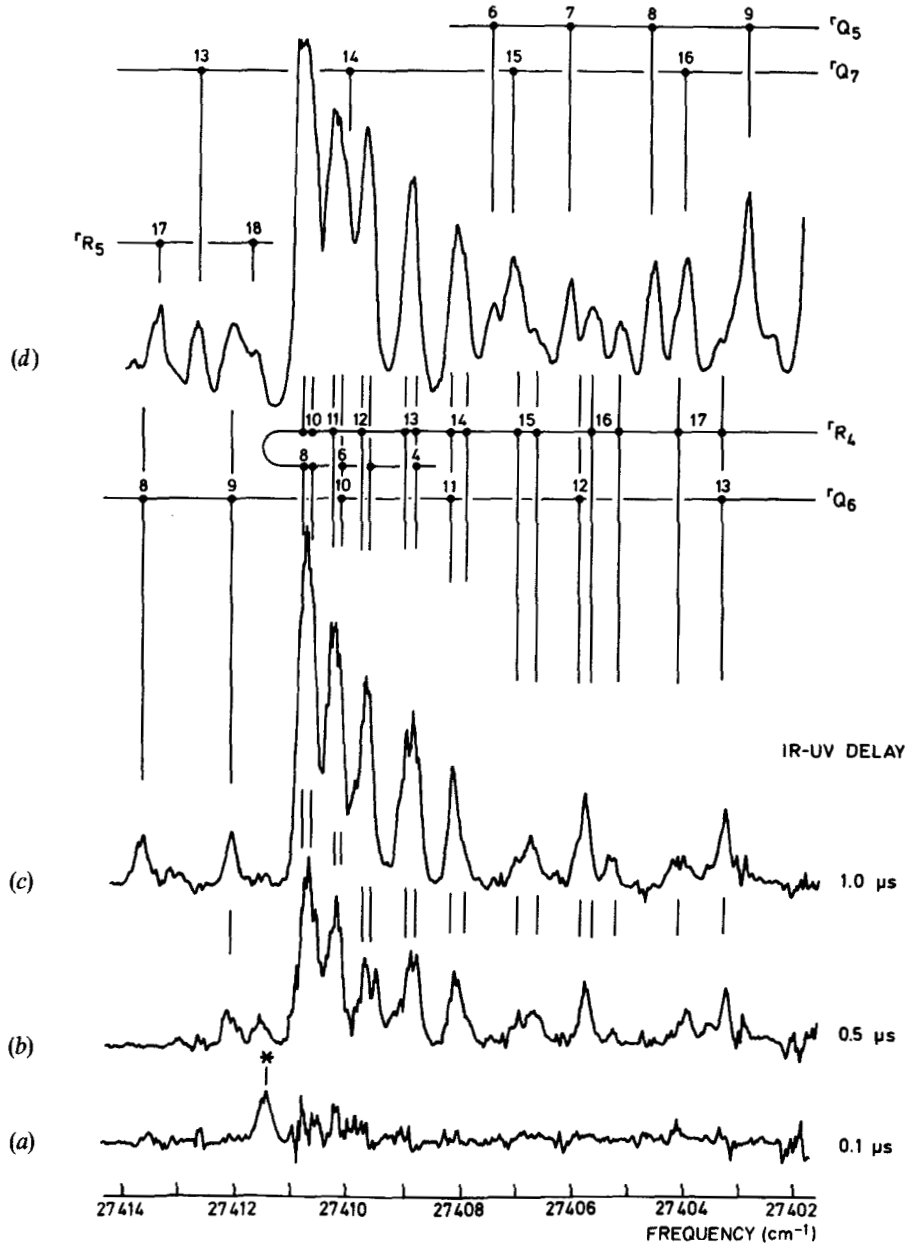

Figure 18. *J*-resolved collision-induced growth of IRUVDR intensity in the vicinity of the $^rR_4$ sub-band of the $\tilde{A}\leftarrow\tilde{X}$ 4_1^0 vibronic band of D_2CO, recorded with a PROBE bandwidth of $\sim 0{\cdot}2\,cm^{-1}$. Note the weak $^tQ_4(11)$ parent peak (asterisked) of the 6_1^0 band. The IRUVDR difference spectra in traces (*a*)–(*c*) have $P_{D_2CO} = 50$ mTorr and D_2CO/D_2CO collision number $z = 0{\cdot}05$, $0{\cdot}25$ and $0{\cdot}5$ respectively. Trace (*d*) is a background LIF excitation spectrum (Bewick 1989).

probability ratio for the 4_1^0- and 6_1^0-bands (Orr 1974, Orr and Haub 1984) is apparent in these spectra: collision-induced growth of integrated intensity in the 4_1^0-band vastly exceeds the nascent intensity in the $^tR_4(11)$ and $^tQ_4(11)$ parent features, prior to rotational relaxation.

The background LIF excitation spectra in figures 17(*e*) and 18(*d*) are provided for comparison. A number of 4_1^0-band features with odd K_a do not appear in the corresponding IRUVDR spectra, because the infrared PUMP excitation prepares only even-K_a states (see figure 7) and the slow rate of interconversion between the *ortho* and *para* modifications of D_2CO prevents odd-$|\Delta K_a|$ transfer. IRUVDR spectra such as those in figures 17(*d*) and 18(*c*), although rotationally relaxed with respect to J, are therefore less congested than the corresponding background spectra.

IRUVDR spectra at a selection of discrete values of IR–UV delay (and hence of collision number z), such as those in figures 16, 17 and 18, have been supplemented by kinetic studies in which the IR–UV delay is scanned continuously with the PROBE dye laser fixed on a single prominent rovibronic transition. A selection of the resulting kinetic curves is presented in figure 19. Comparable kinetic curves recorded with relatively broad dye-laser bandwidth for ^rR sub-band heads (in which J-states are not well resolved) have already appeared in figure 15 (Bewick and Orr 1989a). However, each of those curves arises from population in several (J', K_a')-states of the $v_4 = 1$ manifold, whereas those in figure 19 are J-resolved. The kinetic curves in figure 19 belong to a wide-ranging set comprising 24 curves for individual $v_4 = 1$, (J', K_a') states and 4 curves for RET in $v_6 = 1$, (J, K_a) states (Bewick 1989). It should be noted that the quality of the kinetic data now available is markedly superior to that previously reported (Haub and Orr 1984, 1987) and that there are subtle variations in the growth of the kinetic curves for different (J', K_a')-states reflecting the mechanisms of the simultaneous $\nu_6 \rightarrow \nu_4$ transfer and RET on which they depend. The solid curves in figures 15 and 19 are derived from a rotationally specific kinetic model of $\nu_6 \rightarrow \nu_4$ transfer and RET in D_2CO, which will now be described.

Our detailed kinetic model of rotationally resolved $\nu_6 \rightarrow \nu_4$ transfer in D_2CO employs a kinetic master-equation formalism to compute the flow of population, within the (ν_4, ν_6) rovibrational manifold of D_2CO, following pulsed laser excitation (Bewick and Orr 1989a, Bewick 1989). The approach is similar to (but far more complicated than) that adopted in the context of RET (Bewick *et al.* 1985) and outlined in section 5 above. Figure 20 depicts the situation of interest, represented by 80 $v_6 = 1$ levels (with $K_a = 0, 2, 4$ and 6) and 85 $v_4 = 1$ levels (with $K_a' = 2, 4, 6, 8$ and 10). These levels are coupled by a matrix $\mathbf{\Pi}$ of pseudo-first-order rate constants comprising those for rotational relaxation (with changes of J and/or K_a) and $\nu_6 \rightarrow \nu_4$ vibrational energy transfer. The time profile of the infrared PUMP pulse (typically 150 ns f.w.h.m. with a weak 450 ns tail) is emulated by a histogram of pumping rate constants $\delta\mathbf{\Pi}(t)$ in the manner of our treatment of RET; the rates of both J- and K_a-changing rotational relaxation are consistent with those established in that same investigation (Bewick *et al.* 1985). For kinetic curves recorded over a range of pressures, as in figure 15, an acceptable fit is obtained by assuming that the kinetics are second-order, with no need to include a first-order contribution. This discredits suggestions that the apparently complex pressure dependence of the $\nu_6 \rightarrow \nu_4$ transfer kinetics could derive from a collision-free unimolecular process (Bewick and Orr 1989a).

Bewick and Orr (1989a) have found that the dominant channel of $\nu_6 \rightarrow \nu_4$ transfer in D_2CO/D_2CO collisions is that with $K_a = 4 \rightarrow 6$ and $\Delta J = 0$. The best fit to the experimental kinetic data is obtained with a microscopic rate constant for this channel

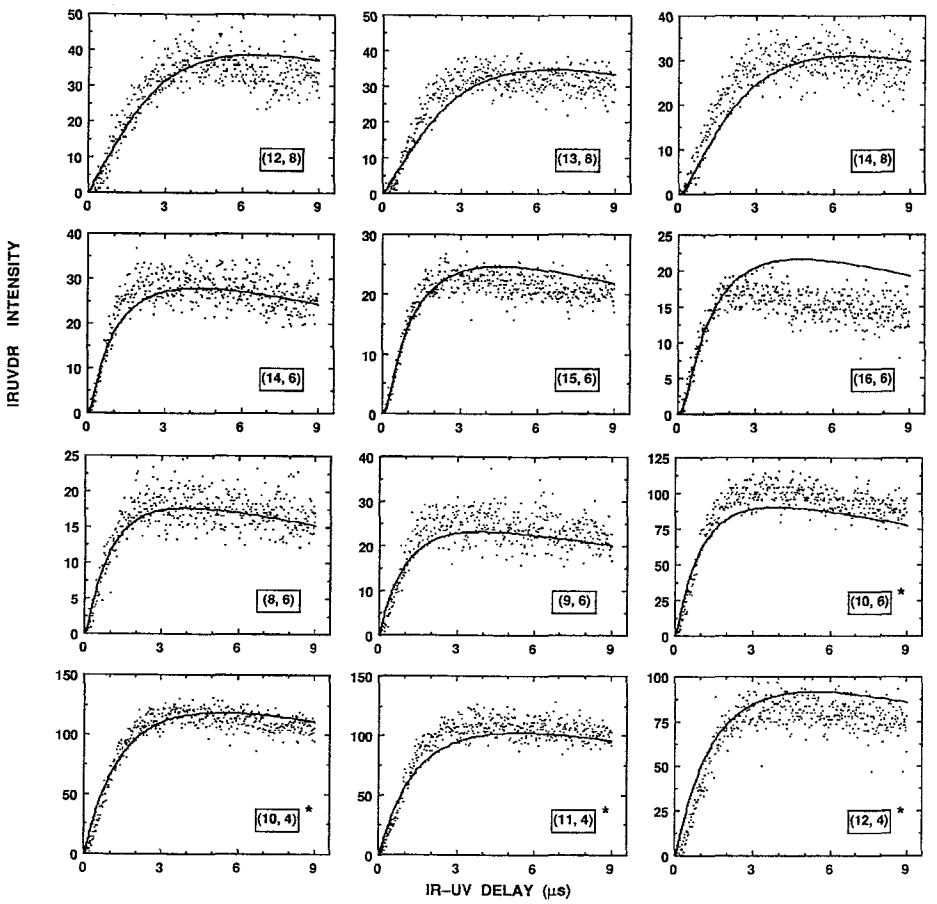

Figure 19. J-resolved IRUVDR kinetic curves measuring growth and decay of population in the $\tilde{X}$, $v_4 = 1$ manifold of D_2CO, arising from excitation by the 10 R(32) CO_2-laser line and subsequent collision-induced $\nu_6 \rightarrow \nu_4$ transfer. The digitally recorded kinetic curves cover a range of (J', K_a')-states and the solid curves are the corresponding computed predictions of the detailed kinetic model. Curves labelled with an asterisk are overlapped by one or more rovibronic transition in the 4_1^0-band spectrum. The abscissa of each plot is the IR–UV delay t, between ultraviolet PROBE and infrared PUMP laser pulses (Bewick 1989).

of $1{\cdot}5\,\mu s^{-1}\,Torr^{-1}$. However, this dominant channel of J-specific rovibrational energy transfer is only one of many contributing significantly to the overall $\nu_6 \rightarrow \nu_4$ transfer mechanism. Other channels include $K_a = 4 \rightarrow 6$ (with $\Delta J = \pm 1$ and ± 2) and the following additional changes of K_a (all with $\Delta J = 0, \pm 1$ and ± 2): $0 \rightarrow 0, 2$ and 4; $2 \rightarrow 0, 2$, 4 and 6; $4 \rightarrow 4$ and 8; $6 \rightarrow 6$ and 8. However, the best fit to the observed kinetic data is obtained when these additional channels are attributed individual state-to-state constants substantially smaller than $1{\cdot}5\,\mu s^{-1}\,Torr^{-1}$ (and never greater than $0{\cdot}4\,\mu s^{-1}\,Torr^{-1}$). In addition, it is found advantageous to scale the rate constants for the dominant $K_a = 4 \rightarrow 6$, $\Delta J = 0$ channel of $\nu_6 \rightarrow \nu_4$ transfer as $\sim J^3$, which is consistent with the predicted functional dependence of the Coriolis-induced $\nu_6 \rightarrow \nu_4$ transfer rate (Haub and Orr 1987).

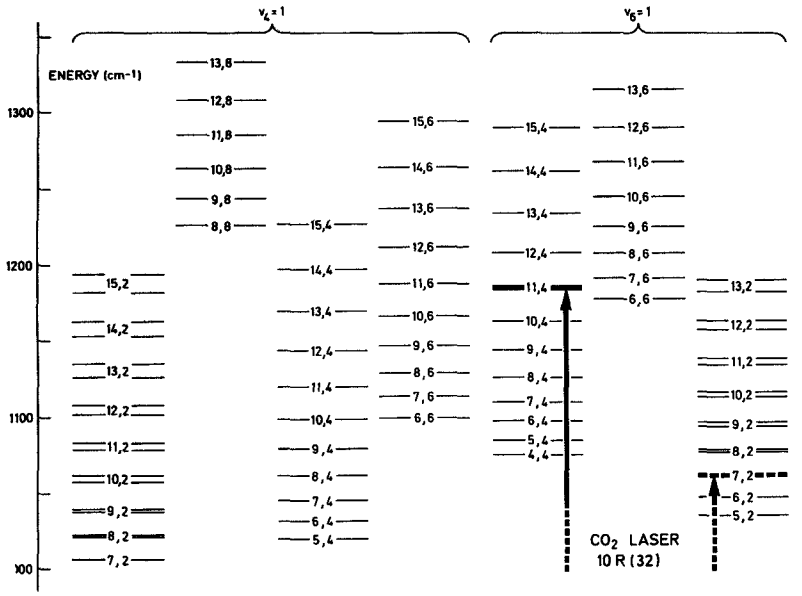

Figure 20. Partial rovibrational energy level diagram for D_2CO, showing states likely to be involved in $v_6 \rightarrow v_4$ collision-induced transfer after initial excitation by the 10 R(32) CO_2-laser line. The energy scale on the ordinate is referred to the zero-point vibrational level.

Various forms of fitting law have been tested, all based on three adjustable parameters fitting the V–V transfer and all satisfying detailed balance. The only uniquely satisfactory feature of such fitting laws is the dominant $K_a=4\rightarrow6$, $\Delta J=0$ channel of $v_6\rightarrow v_4$ transfer. The quality of the fit to the experimental kinetic data is well represented by figures 15 and 19. Other fitting laws with less rotational (J, K_a)-state specificity provide a less adequate overall fit to the experimental kinetic curves. A remarkably poor fit is provided by an exponential-gap fitting law, in which the V–V transfer rates are scaled simply according to the energy gap $|\Delta E|$ between the initial and final rovibrational states, without any consideration of angular momenta. This indicates that the rotational identity of the initial and final states participating in $v_6\rightarrow v_4$ transfer is crucially important.

It is evident from this kinetic modelling that rotationally-selective channels of $v_6\rightarrow v_4$ transfer prevail in the case of D_2CO/D_2CO collisions, with the $K_a=4\rightarrow6$, $\Delta J=0$ channel predominant. This conclusion is entirely consistent with the previous predictions of Haub and Orr (1987), on the basis of dipole–dipole interactions treated in the first order of the Born approximation, as outlined in section 6. In simple terms, long-range D_2CO/D_2CO collisions have the effect of coupling the rovibrational quantum numbers K_a, v_4 and v_6, whereas J remains uncoupled as if it belongs to a separate dynamical system. This conclusion is consistent with the useful classical perspective recently provided by Parson (1988, 1989, 1990).

The detailed kinetic modelling approach provides a reliable estimate of the intrinsic rate of rotationally selective, collision-induced $v_6\rightarrow v_4$ transfer in D_2CO (separated from the accompanying blend of J- and K_a-changing rotational relaxation processes). The microscopic state-to-state rate constants for rotationally-resolved $v_6\rightarrow v_4$ transfer are remarkably efficient by the standards normally applied to V–V transfer. This,

together with the rotational selectivity favouring $K_a = 4 \rightarrow 6$, $\Delta J = 0$ processes, confirms the role of Coriolis coupling in promoting such processes, as previously proposed by Haub and Orr (1987).

The above results provide evidence that molecules can 'remember' their initial rotational state after undergoing $\nu_6 \rightarrow \nu_4$ transfer. The evidence is indirect, however, for the V–V transfer is experimentally inseparable from accompanying J-changing RET, as demonstrated by figures 17 and 18. The rotationally specific channels of $\nu_6 \rightarrow \nu_4$ transfer in D_2CO/D_2CO collisions can only be inferred by the above kinetic modelling procedures. A more direct demonstration of rotationally selective $\nu_6 \rightarrow \nu_4$ transfer is made possible by choosing a foreign-gas collision partner M, such that D_2CO/M collisions enhance the efficiency of V–V transfer relative to J-changing RET. Such a situation pertains to D_2CO/N_2O collisions, as is illustrated in figure 21 (Bewick 1989). Traces (*a*)–(*c*) show IRUVDR difference spectra in the vicinity of the $K'_a = 4$ ^rR sub-band head in the 365 nm 4_1^0 vibronic band of D_2CO, indicating the evolution of population in various J-states of the $v_4 = 1$, $K'_a = 4$ manifold, as in figure 18. The difference from figure 18 is that figures 21 (*b*) and (*c*) show the effect of increasing the D_2CO/N_2O collision number z_{N_2O}, with the rate of D_2CO self-collisions maintained at a negligible value. It is significant to note that the (asterisked) 6_1^0 $^tQ_4(11)$ parent peak shows little decay under these conditions, demonstrating that rotational relaxation of the initially prepared $v_6 = 1$, $J = 11$, $K_a = 4$ rovibrational state is minimal. We therefore infer that the observed IRUVDR features in traces (*b*) and (*c*) indicate the nascent distribution of J-state population in the $K'_a = 4$ and 6 manifolds of D_2CO, following $\nu_6 \rightarrow \nu_4$ transfer induced by collisions with N_2O but prior to appreciable collision-induced rotational relaxation.

It is evident that the rotationally-selective channels of $\nu_6 \rightarrow \nu_4$ transfer in D_2CO/N_2O collisions are relatively widespread compared to those for D_2CO/D_2CO collisions, where the dominant channel of $\nu_6 \rightarrow \nu_4$ transfer corresponds to $K_a = 4 \rightarrow 6$ and $\Delta J = 0$. By contrast, any model of $\nu_6 \rightarrow \nu_4$ transfer in D_2CO/N_2O collisions must invoke the shorter-range portion of the intermolecular potential to account for the more widespread distribution of nascent population in the (J', K'_a)-states of the $v_4 = 1$ manifold. Apparently, it is no longer appropriate to associate J with a dynamical system separate from that to which the set (K_a, v_4, v_6) belongs, nor to regard $K_a = 4 \rightarrow 6$ as the sole dominant $\nu_6 \rightarrow \nu_4$ transfer channel. It is also evident that foreign-gas collisions are able to narrow the gap between the rates of V–V transfer and rotational relaxation, thereby enhancing the degree of rotational specificity in rovibrational energy transfer. Work is in progress to model IRUVDR kinetic measurements of D_2CO/N_2O mixtures (Bewick *et al.* 1989).

The above results run contrary to the normal expectation that rotational scrambling should erase any 'memory' of the initially prepared rotational quantum number J. It is now apparent that V–V transfer tends to favour certain specific rotational channels, that such channels can be observed directly in special circumstances such as $\nu_6 \rightarrow \nu_4$ transfer in D_2CO molecules, and that foreign-gas collisions may play subtle roles in controlling rotational selectivity. This last theme is explored further in the next section.

8. The effect of foreign-gas collisions of energy transfer in D_2CO

The preceding example, illustrated in figure 21, suggests that there is much to be learned about energy transfer resulting from collisions of D_2CO with atoms or molecules M of a foreign gas. This enables the collisional conditions, particularly the

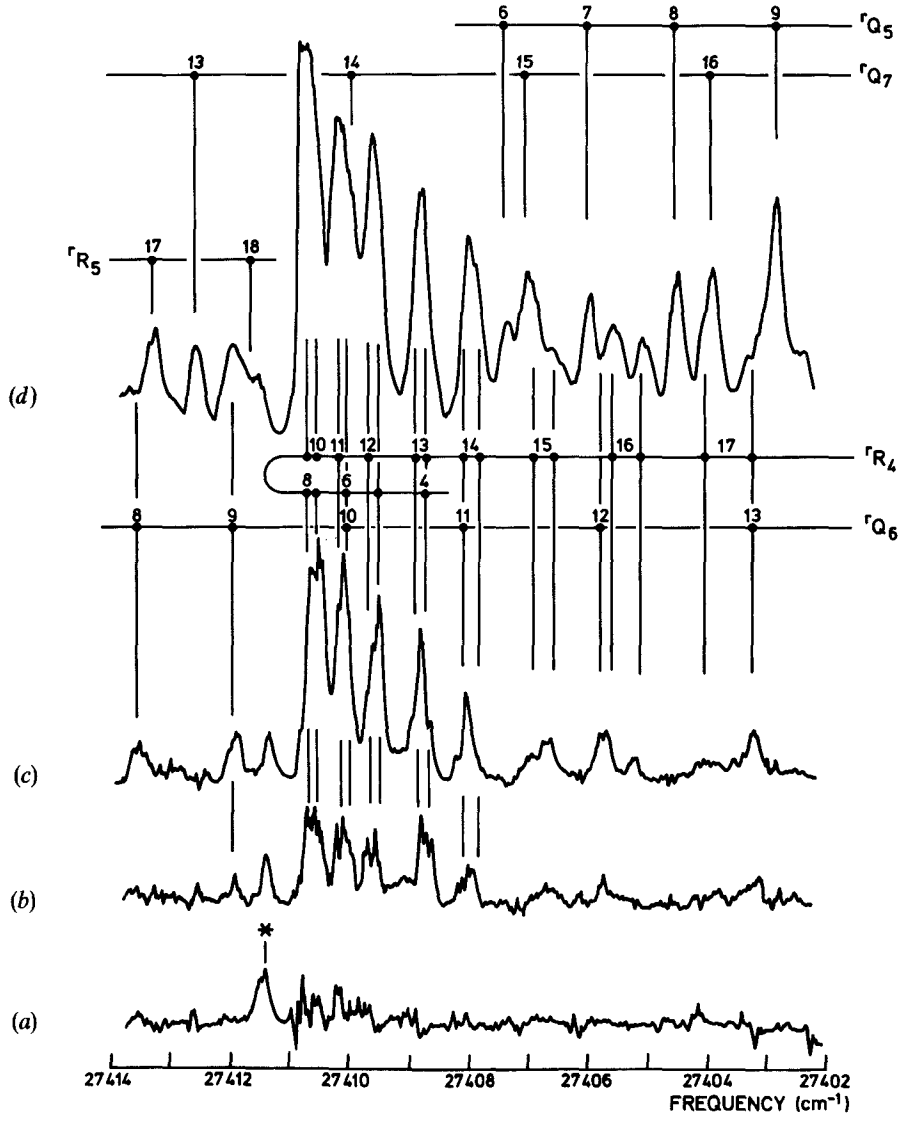

Figure 21. Fluorescence excitation spectra demonstrating the effect of D_2CO/N_2O collisions on rotationally selective V–V transfer into the ($v_4 = 1$, $K'_a = 4, 6$) rovibrational manifolds of D_2CO. Traces (*a*)–(*c*) are IRUVDR difference spectra obtained with the CO_2 10 R(32) laser line, an IR–UV delay of 100 ns and the following collisional conditions: (*a*) $P_{N_2O} = 0$, $z_{N_2O} = 0$; (*b*) $P_{N_2O} = 300$ mTorr, $z_{N_2O} = 0{\cdot}29$; (*b*) $P_{N_2O} = 635$ mTorr, $z_{N_2O} = 0{\cdot}60$. The D_2CO partial pressures are: (*a*) $P_{D_2CO} = 50$ mTorr; (*b*), (*c*) $P_{D_2CO} = 30$ mTorr; the D_2CO/D_2CO collision number z is therefore 0·05 or less. Trace (*d*) is a background LIF excitation spectrum, with $P_{D_2CO} = 50$ mTorr and the instrumental gain halved relative to traces (*a*)–(*c*) (Bewick 1989).

intermolecular potential and the availability of quasi-resonant channels, to be varied by choice of collision partner M. The general situation, with which our time-resolved IRUVDR experiments are then concerned, is of the form

$$D_2CO(V;R)+M\rightarrow D_2CO(V';R')+M, \tag{4}$$

where V, V′ denote particular vibrational levels (either $v_4=1$ or $v_6=1$), with V = V′ in the case of RET and V ≠ V′ in the case of $v_6\rightarrow v_4$ transfer as in (2), and R, R′ denote corresponding rotational states (J, K_a, K_c).

Variation of the collision partner M also helps us to resolve ambiguities in energy transfer mechanisms which arise in the case of self-collisions. In D_2CO/D_2CO collisions, D_2CO molecules serve both as state-selected species and (in the $v=0$ vibronic ground state) as collision partner M. There are then two possible mechanisms for the collision-induced energy transfer process represented by (4). It could be *intramolecular*, with the state-selected D_2CO molecule remaining excited (albeit in a different rovibrational state) after energy transfer has occurred:

$$D_2CO(V;R)+\underline{D_2CO}\,(v=0;R'')\rightarrow D_2CO(V';R')+\underline{D_2CO}\,(v=0;R'''). \tag{5}$$

where the collision-partner molecule has been distinguished hypothetically by underlining. On the other hand, the process (4) could be *intermolecular*, where the PUMP excitation originally deposited in the state-selected D_2CO molecule migrates to the collision-partner D_2CO molecule during a D_2CO/D_2CO collision:

$$D_2CO(V;R)+\underline{D_2CO}\,(v=0;R'')\rightarrow D_2CO(v=0;R''')+\underline{D_2CO}\,(V';R'), \tag{6}$$

Although the intramolecular mechanism (5) has been favoured on intuitive grounds in most of our IRUVDR studies on D_2CO/D_2CO collisions (see sections 5–7 above), the intermolecular mechanism (6) cannot be discounted on the basis of that evidence alone. Indeed, both (5) and (6) could be proceeding simultaneously. By contrast, the energy-transfer process represented by (4) in the case where $M\neq D_2CO$ is intrinsically intramolecular, since only one D_2CO molecule is involved and its rovibrational state is specified before and after the collision. If the rate constants for a particular process are of comparable magnitude with both D_2CO/D_2CO and D_2CO/M collisions, then it can be inferred that the D_2CO/D_2CO case is predominantly intramolecular.

Bewick *et al.* (1988) have examined the dependence of J-changing RET in D_2CO on foreign-gas collision partner M, by IRUVDR studies of rotational relaxation out of the initially prepared $\tilde{X}$, $v_4=1$, $(J, K_a)=(18, 11)$ rovibrational state. Figure 22 presents a survey of IRUVDR difference spectra for a variety of collision partners ($M=N_2O$, N_2, Ar, He, as well as D_2CO itself); D_2CO/M collision numbers z_M are as indicated. These spectra should be compared with results for D_2CO/D_2CO collisions in pure formaldehyde vapour, as in figure 8. It is apparent from figure 8 (*b*) that rotational equilibration of J-states within the $\tilde{X}$, $v_4=1$, $K_a=11$ manifold is virtually complete after a single D_2CO/D_2CO hard-sphere collision interval. The range of foreign-gas collision partners presented in figure 22 shows a gradation of behaviour between the extremes of J-changing RET in D_2CO/He and D_2CO/N_2O collisions. All of the collision partners studied are much less efficient in redistributing rotational population than are D_2CO/D_2CO collisions: even with collision number $z_M\approx 2{\cdot}0$ and a dipolar collision partner M such as N_2O, the $^rR_{11}(18)$ parent peak remains prominent and rotational equilibration still has a long way to go. A wider range of D_2CO/N_2O collision numbers is represented in the IRUVDR difference spectra of figure 23, with percentage estimates of the population surviving in the parent rovibrational state

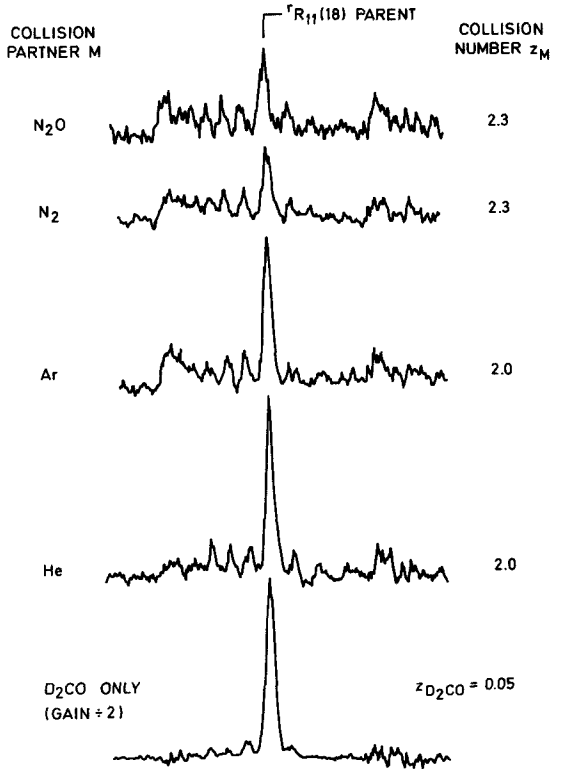

Figure 22. IRUVDR difference spectra for pure D_2CO and a series of D_2CO/M mixtures, where M is a foreign gas as listed, recorded in the same spectral region as those of figure 8 with the 10 R(28) CO_2-laser line and an IR–UV delay of 0·25 μs. The D_2CO/M collision numbers z_M are all maintained at ~ 2. The spectra show the different patterns of J-changing RET out of the $\tilde{X}$, $v_4 = 1$, $(J, K_a) = (18, 11)$ parent level, as a function of collision partner M (Bewick *et al.* 1988).

relative to the D_2CO/D_2CO reference spectrum as indicated (Bewick 1989). N_2O serves as a collision partner in which electric dipole–dipole interactions with D_2CO are still expected to dominate, but its electric dipole moment (0·17 debye) is substantially smaller than that of D_2CO (2·34 debye) and it lacks the property of 'rotational resonance' (Oka 1967, 1973) inherent in D_2CO self-collisions. As a general rule, J-changing RET in D_2CO/M collisions tends to be spread over a wider range of $|\Delta J|$ than in the D_2CO/D_2CO case, where there is a propensity for $|\Delta J| = 1$ transfer. This tendency becomes more pronounced as M moves through the series: N_2O, N_2, Ar, He; this is consistent with the relative weakness and shorter range of a D_2CO/(atom) intermolecular potential, compared to the strongly dipolar character of D_2CO/D_2CO interactions (Bewick *et al.* 1988). Detailed studies of such RET effects have not been undertaken, but the general trend is evident from the preliminary survey which has been made. There is insufficient evidence here to establish whether or not D_2CO/D_2CO collisions have a strong intermolecular component of type (6) in their J-changing RET. However, it is generally assumed on theoretical grounds that J-changing RET is predominantly intramolecular, as in (5).

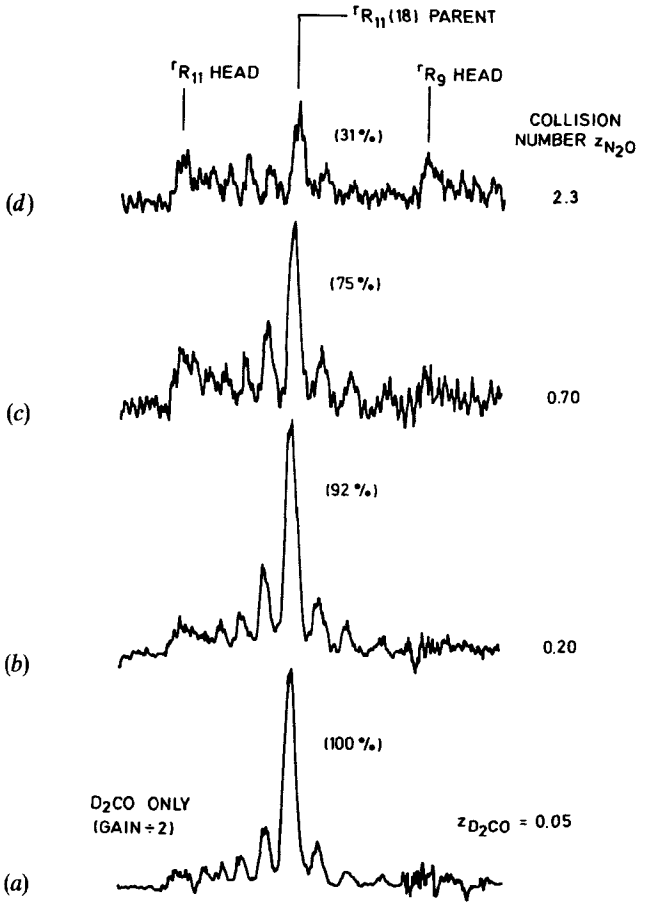

Figure 23. IRUVDR difference spectra, similar to those in figure 22, for pure D_2CO (*a*) and a series of D_2CO/N_2O mixtures (*b*), (*c*), (*d*), recorded with the 10 R(28) CO_2-laser line, an IR–UV delay of 0·25 μs, and D_2CO/N_2O collision numbers z_{N_2O} as indicated. The fraction of population remaining in the $\tilde{X}$, $v_4=1$, $(J, K_a)=(18, 11)$ parent rovibrational level, corrected for collisional quenching effects, is indicated in parentheses (Bewick 1989).

Bewick and Orr (1989b) have also studied the effect of foreign-gas collisions on D_2CO and have reached a more positive conclusion concerning the distinction between intramolecular and intermolecular mechanisms. Figure 24 presents a set of relevant survey IRUVDR difference spectra showing $v_6 \rightarrow v_4$ transfer in D_2CO, as a result of interactions with a variety of collision partners (He, Ar, CH_4, N_2, N_2O, as well as D_2CO itself). As in figure 14, this illustrates the collision-induced intensity of prominent features in the 4_1^0 hot band associated with rovibrational states having $v_4=1$ and $K'_a=2, 4, 6$ and 8. In the case of D_2CO/D_2CO collisions, the collision-induced features have grown within less than two gas-kinetic collision intervals from the null values observed when the IR–UV delay t is zero (see figure 14 (*a*)) to become relatively intense, as shown by the identical traces in figures 14 (*c*) and 24 (*f*). The corresponding IRUVDR difference spectra, for mixtures of D_2CO with a range of collision partners M, are shown in figures 24 (*a*)–(*e*). All are recorded with a common collision number z_M

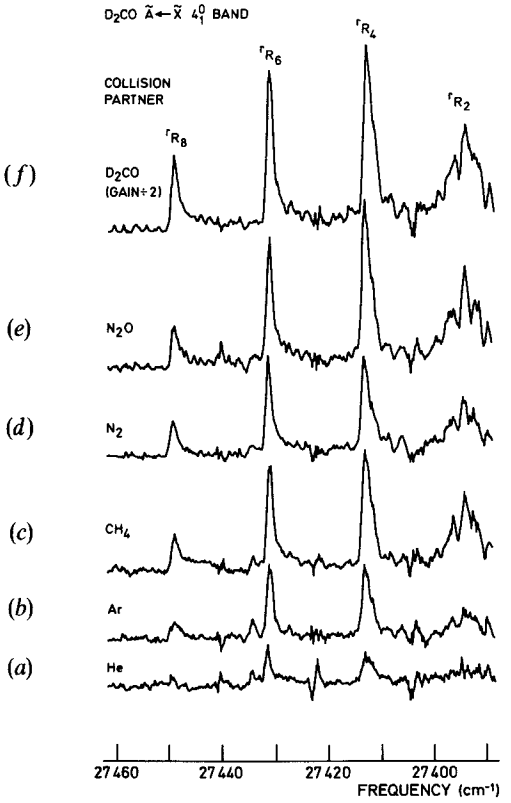

Figure 24. IRUVDR difference spectra of the 365 nm $\tilde{A}\leftarrow\tilde{X}$ 4_1^0 band of D_2CO, recorded with the CO_2 10R(32) laser line and a variety of collision partners M (M = He, Ar, CH_4, N_2, N_2O and D_2CO). The optical bandwidth of the UV PROBE dye laser is $\sim 0{\cdot}7\,cm^{-1}$ f.w.h.m. and the collision number z_M for D_2CO/M hard-sphere collisions is maintained throughout at 1·6, by control of P_M and the IR–UV delay t. For traces (*a*)–(*e*), $P_{D_2CO} = 30$ mTorr, $t = 250$ ns and $z_{D_2CO} = 0{\cdot}08$, whereas trace (*f*) has been recorded with $P_{D_2CO} = 50$ mTorr, $t = 3{\cdot}0\,\mu s$, $z_{D_2CO} = 1{\cdot}6$ and a twofold reduction in instrumental gain. The spectra should be compared with those in figure 14. They show qualitatively how the efficiency of $\nu_6 \rightarrow \nu_4$ transfer in D_2CO increases through the series M = He,..., D_2CO (Bewick and Orr 1989b).

of 1·6 for D_2CO/M hard-sphere collisions and with an instrumental gain that is only a factor of two greater than that used to record figure 24(*f*). It is apparent that the intensity of the collision-induced IRUVDR features, and hence the V–V transfer efficiency, increases gradually through the series He, Ar, N_2, CH_4, N_2O and approaches that of the case where M = D_2CO. These spectra alone indicate that collisions of D_2CO with foreign-gas partners are not markedly less efficient in promoting V–V transfer than are self-collisions. This in turn suggests qualitatively that $\nu_6 \rightarrow \nu_4$ vibrational transfer in D_2CO/D_2CO collisions proceeds primarily through an intramolecular mechanism as in (5), rather than through an intermolecular exchange of vibrational quanta as in (6).

A more detailed view of $\nu_6 \rightarrow \nu_4$ vibrational transfer in mixtures of D_2CO and N_2O has been obtained by recording *J*-resolved IRUVDR difference spectra such as those

already presented in figures 21(*a*)–(*c*), showing collision-induced evolution of population in individual J-states of the $\tilde{X}$, $v_4=1$, $K'_a=4$ manifold (Bewick 1989). As the D_2CO/N_2O collision number z_{N_2O} is increased from 0·29 to 0·60, the collision-induced IRUVDR intensity grows accordingly and distributes itself over an increasingly wide range of rotational states. Corresponding spectra for the $v_4=1$, $K'_a=6$ manifold have been reported by Bewick and Orr (1989b). Figures 17 and 18 show IRUVDR spectra of similar quality in the case of D_2CO/D_2CO collisions. As has already been noted in section 7 and borne out by figures 22 and 23, the rate of J-changing rotational relaxation is very much less efficient in the case of D_2CO/N_2O collisions, than in D_2CO/D_2CO collisions. This enables IRUVDR spectra such as figures 21 (*b*) and (*c*) to give a direct view of the (J', K'_a)-resolved nascent distribution of population arising from $\nu_6 \rightarrow \nu_4$ vibrational transfer in D_2CO/N_2O collisions. This is found to cover a much wider range of rotational (J', K'_a)-states of the $v_4=1$ manifold than is inferred from modelling of $\nu_6 \rightarrow \nu_4$ transfer in D_2CO/D_2CO collisions, where the channel with $K_a=4\rightarrow6$ and $\Delta J=0$ predominates.

Bewick and Orr (1989b) have measured and analyzed the kinetics of $\nu_6 \rightarrow \nu_4$ vibrational energy transfer in mixtures of D_2CO and N_2O, using a variant of the approach applied elsewhere to pure D_2CO vapour (Haub and Orr 1987, Bewick *et al.* 1988). A novel aspect of this approach comprises separation of rate constants for $\nu_6 \rightarrow \nu_4$ transfer in D_2CO/D_2CO and D_2CO/N_2O collisions through kinetic experiments in which the mole fraction X of D_2CO in the gas mixture is varied. Typical kinetic results for the prominent $^rR_6$ sub-band head in the 4^0_1 band (thereby monitoring population in states with $v_4=1$, $K'_a=6$ and $J'\approx6$–11) are shown in figure 25. Here, the fitted kinetic curves are supposed to be of the triple-exponential form

$$I(t) = -A\exp(-t/\tau_r) + B\exp(-t/\tau_f) + (A-B)\exp(-t/\tau_s), \tag{7}$$

where $I(t)$ is the IRUVDR intensity expressed as a function of IR–UV delay time t and $\tau_s \gg \tau_r, \tau_f$. The kinetic data are fitted by a least-squares regression with four adjustable parameters: the two amplitudes (A, B) and the time constants for the fast rise (τ_r) and fall (τ_f) components of the signal. The slow decay term (time constant τ_s) is fixed uniformly by inspection. The dependence of the time constants τ_s, τ_r and τ_f on mole fraction X and on total pressure P is assumed to be ideal:

$$(P\tau_i)^{-1} = Xk_i(D_2CO/D_2CO) + (1-X)k_i(D_2CO/N_2O), \tag{8}$$

where i = s, r or f and the quantities $k_i(D_2CO/M)$ are second-order rate constants for processes induced by D_2CO/M collisions. Plots of $(P\tau_i)^{-1}$ as a function of mole fraction X enable the second-order rate constants $k_i(D_2CO/N_2O)$ and $k_i(D_2CO/D_2CO)$ to be evaluated. A typical example of such plots for the $v_4=1$, $K'_a=6$ manifold is presented in figure 26, confirming that the ideal form of fitting function assumed in (8) is adequate.

The foregoing procedure of kinetic analysis has been applied by Bewick and Orr (1989b) to an extensive body of IRUVDR kinetic results for D_2CO/N_2O gas mixtures, monitoring each of the three most prominent ^rR sub-band head features which appear in figure 24 (thereby covering a range of rotational states with $J'\approx6$–11 and $K'_a=4, 6$ and 8). The most remarkable aspect of this kinetic analysis is that collision-induced $\nu_6 \rightarrow \nu_4$ transfer in D_2CO remains extraordinarily efficient with N_2O as a collision partner: values of $k_{r/f}(D_2CO/N_2O)$ are never less than a factor of two below the hard-sphere collision rate and never less than a factor of five below the corresponding values of $k_{r/f}(D_2CO/D_2CO)$. The preference which Coriolis-induced $\nu_6 \rightarrow \nu_4$ transfer shows for the $K_a=4\rightarrow6$ channel in the case of D_2CO/D_2CO collisions does not appear to be as pronounced in the case of D_2CO/N_2O collisions, which again highlights the especially

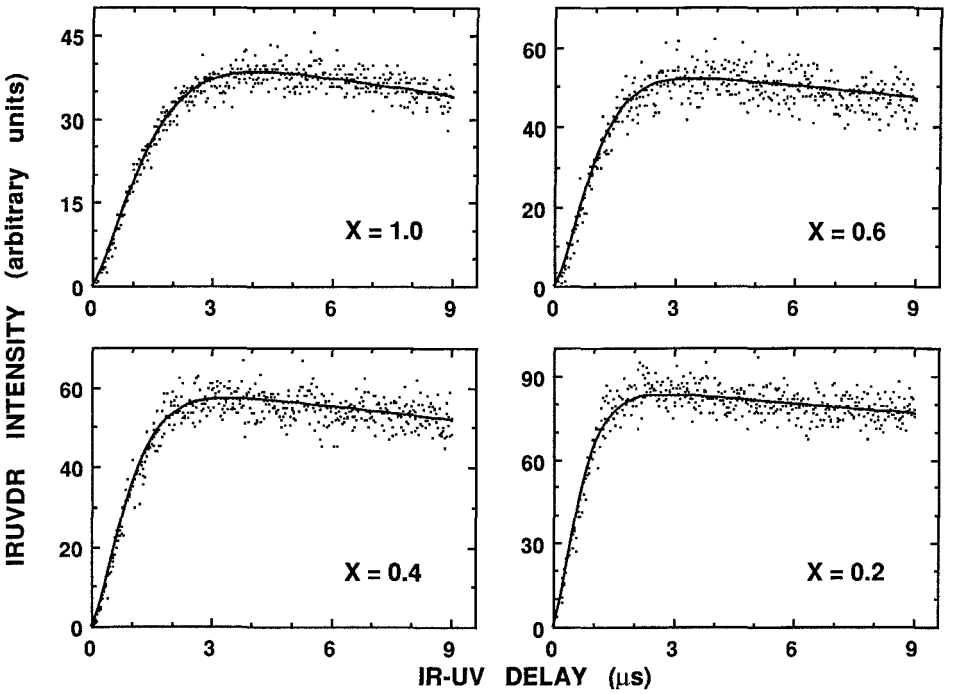

Figure 25. Representative kinetic curves for a variety of D_2CO/N_2O mixtures, showing the IRUVDR intensity $I(t)$ due to rovibrational levels of D_2CO specified by $v_4 = 1$, $K'_a = 6$ and $J' \approx 6$–11, following excitation by the 10 R(32) CO_2 laser line and collision-induced $v_6 \rightarrow v_4$ transfer. The partial pressure P_{D_2CO} is 30 mTorr and P_{N_2O} is varied to yield the D_2CO mole fractions X listed. The data are fitted to a triple-exponential function, as defined by (7) (Bewick and Orr 1989b).

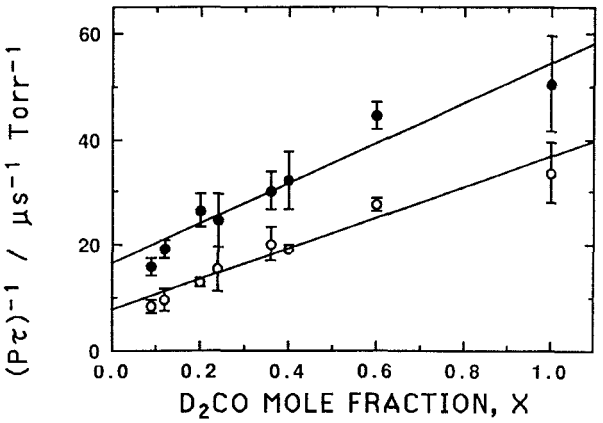

Figure 26. Dependence on mole fraction X, in a series of D_2CO/N_2O mixtures, of fitted kinetic eigenvalues τ_r^{-1} and τ_f^{-1} for collision-induced $v_6 \rightarrow v_4$ transfer into the ($v_4 = 1$, $K'_a = 6$) manifold of D_2CO. The data are plotted according to (8), yielding intercepts at $X = 1$ and 0 which correspond to the second-order rate constants $k_{r/f}(D_2CO/D_2CO)$ and $k_{r/f}(D_2CO/N_2O)$ respectively. Vertical bars denote the spread of experimental data points derived from fitting to available kinetic curves (of which those in figure 25 are typical) for a single value of X (Bewick and Orr 1989b): (●), decay; and (○), rise.

high rotational selectivity in the case of D_2CO self-collisions. The above differences between $k_{r/f}(D_2CO/D_2CO)$ and $k_{r/f}(D_2CO/N_2O)$ are relatively small, especially when it is recognized that the electric dipole moment of N_2O is an order of magnitude smaller than that of D_2CO so that the strength of long-range dipole–dipole interactions in the D_2CO/D_2CO case greatly exceeds that in the D_2CO/N_2O case. As has already been proposed, an appreciable second-order rate constant $k_{r/f}(D_2CO/N_2O)$ implies that the collision-induced intramolecular mechanism (5) for $\nu_6 \rightarrow \nu_4$ transfer in D_2CO is intrinsically efficient. It then follows that $\nu_6 \rightarrow \nu_4$ transfer in D_2CO/D_2CO collisions proceeds primarily through an intramolecular pathway as in (5), as opposed to an intermolecular process in which vibrational excitation migrates from one D_2CO molecule to another as in (6).

It should be noted that the above second-order rate constants $k_{r/f}(D_2CO/M)$ are phenomenological and representative only of *macroscopic* rate processes. They do not necessarily correlate directly with the actual *microscopic* state-to-state rate processes responsible for the detailed mechanism of $\nu_6 \rightarrow \nu_4$ transfer in D_2CO. This association of microscopic energy-transfer channels can be reliably established only by detailed kinetic modelling of observed kinetic data. This has been accomplished in the cases of D_2CO/D_2CO collisions for J-changing RET (Bewick *et al.* 1988) and of rotationally resolved $\nu_6 \rightarrow \nu_4$ transfer (Bewick and Orr 1989a, Bewick 1989), as demonstrated in sections 5 and 7 respectively. The microscopic state-to-state rate constants extracted in this way are typically much smaller than the phenomenological macroscopic rate constants fitted to the observed kinetics: by a factor of ~ 5 for J-changing RET and ~ 20 for $\nu_6 \rightarrow \nu_4$ transfer. This latter discrepancy reflects the complex, multichannel nature of the $\nu_6 \rightarrow \nu_4$ transfer mechanism and lessens the appropriateness of fitting a simple functional form to the experimental kinetic data, as in figure 24. Nevertheless, the fitting of a triple-exponential curve to complex kinetic data remains a useful preliminary analysis procedure, to indicate the cumulative order of magnitude of contributing state-to-state processes and (as in figure 26) in registering trends in the state-to-state kinetics of D_2CO/(foreign gas) collisions as a function of mole fraction. Work is still in progress (Bewick *et al.* 1989) to extend our detailed kinetic modelling treatment to accommodate the extra dimension of D_2CO/D_2CO and D_2CO/(foreign gas) collisions competing over a range of mole fractions.

The foregoing discussion has been confined largely to the relative collisional efficiencies and state-specific channels of J-changing RET and $\nu_6 \rightarrow \nu_4$ transfer in D_2CO/N_2O collisions, compared to those in D_2CO/D_2CO collisions. Comparable results are also available from IRUVDR studies of D_2CO/Ar collisions (Bewick *et al.* 1985, Bewick 1989) and these have been modelled in terms of an approximate coupled-channel theory by Peet and Clary (1986). The available evidence indicates that the efficiency of $\nu_6 \rightarrow \nu_4$ transfer in D_2CO/M collisions is not severely degraded when foreign-gas collision partners M are substituted for D_2CO, as was inferred on a cursory basis from figure 24. The intramolecular type of V–V transfer process, which prevails intrinsically when $M \neq D_2CO$, can therefore be inferred also to predominate in the case of self-collisions, when $M = D_2CO$. Intermolecular exchange of ν_6 and ν_4 vibrational quanta between colliding D_2CO molecules might also occur, but such processes do not appear to be prominent. The accumulated results suggest that D_2CO molecules, undergoing $\nu_6 \rightarrow \nu_4$ vibrational transfer induced by a foreign-gas collision partner such as H_2O or Ar, can effectively 'remember' their initial rotational state (since rotational scrambling is minimal) and thereby enable the rotationally-specific channels of $\nu_6 \rightarrow \nu_4$ transfer to be observed directly.

9. The story so far...

In bringing this story to a conclusion, it is fitting to point out the broad scope of spectroscopic and energy-transfer applications which ten years' IRUVDR experiments have revealed. Major achievements in the context of D_2CO have already been reviewed: spectroscopic details in section 4, J-changing rotational relaxation in section 5, Coriolis-assisted $\nu_6 \rightarrow \nu_4$ vibrational transfer in sections 6 and 7, and the subtleties of D_2CO/(foreign gas) collisions in section 8. Parallel IRUVDR studies of HDCO (Orr and Nutt 1980, Orr and Haub 1984, Haub and Orr 1987) have not been emphasized, in the interests of brevity.

Table 2 summarizes typical values of the microscopic state-to-state rate constant deduced from detailed kinetic modelling of RET and $\nu_6 \rightarrow \nu_4$ vibrational transfer, as discussed in sections 5 and 7 respectively. The results are restricted at this state to D_2CO/D_2CO collisions, since modelling of kinetic data for D_2CO/(foreign gas) collisions is not yet complete (Bewick *et al.* 1989). Even for D_2CO/D_2CO collisions, moreover, there are still deficiencies in the information available.

Several additional applications of IRUVDR in D_2CO have not been discussed so far, principally because they do not present as coherent and well understood a story as the topics reviewed above. These additional studies have a bearing on mechanistic aspects of RET, on the nature of the infrared excitation process itself, on the role of collisions in promoting molecules up the vibrational 'ladder' of a particular mode, and on the laser photochemical implications thereof. We therefore conclude with a brief

Table 2. A summary of typical microscopic state-to-state rate constants deduced from detailed kinetic modelling of rotational energy transfer (RET) and $\nu_6 \rightarrow \nu_4$ vibrational transfer processes in D_2CO/D_2CO collisions, as discussed in sections 5 and 7 respectively.

Type of energy-transfer process	Transfer channel(s)	Microscopic state-to-state rate constant ($\mu s^{-1}\,Torr^{-1}$)	Collisional efficiency†	Source of information on rate constants
Hard-sphere collisions	—	10	1·0	$d = 4{\cdot}0$ Å, $T = 300$ K
J-changing RET‡	$\Delta J = \pm 1$	25	2·5	Bewick *et al.* (1988)
	$\Delta J = \pm 2$	7	0·7	
K_a-changing RET§	$\Delta K_a = \pm 2$, with $\Delta J = 0$	7	0·7	Bewick *et al.* (1988) Bewick (1989)
K_c-changing RET	$\Delta K_c = \pm 1$, with $\Delta J = \Delta K_a = 0$	See discussion in section 9		Orr *et al.* (1981) Bewick *et al.* (1988)
$\nu_6 \rightarrow \nu_4$ transfer¶	$K_a = 4 \rightarrow 6, \Delta J = 0$	1·5	0·15	Bewick and Orr (1989a)
	Other channels	$\leqslant 0{\cdot}4$	$\leqslant 0{\cdot}04$	Bewick (1989)

† The collisional efficiency is defined arbitrarily as the ratio of the second-order rate constant of interest to the corresponding gas-kinetic (hard-sphere) collision rate, calculated with the values of collision diameter d and temperature T listed in the first row of the table.

‡ Based on an energy-gap model of RET from the $\tilde{X}$, $v_4 = 1$, $(J, K_a) = (18, 11)$ state of D_2CO.

§ Based on kinetic modelling of simultaneous RET and $\nu_6 \rightarrow \nu_4$ vibrational transfer in D_2CO (Bewick, 1989); the results contradict earlier assumptions in the context of RET (see text).

¶ Based on kinetic modelling of $\nu_6 \rightarrow \nu_4$ vibrational transfer in D_2CO, as discussed in section 7; note that fitted macroscopic rate constants are considerably larger, owing to the multichannel nature of the mechanism involved (see discussion in section 8).

examination of some incompletely understood experimental results in this domain, to suggest that the full story might not yet have been told.

The mechanism of collision-induced K_a-changing RET in D_2CO is not yet well understood, although recent rovibrational kinetic modelling by Bewick (1989) indicates that this has propensity rules which favour even-numbered changes of K_a and zero (or very small) simultaneous changes of J; this is contrary to earlier expectations (Bewick *et al.* 1988) that K_a-changing RET would tend to favour quasi-resonant channels with no constraints on $|\Delta J|$. Even-$|\Delta K_a|$ changes satisfy the conservation of *ortho/para* nuclear-spin character as discussed in section 4. Bewick *et al.* (1988) have shown that quite large even-numbered changes of K_a (e.g. from $K_a = 11$ to 3, as in figure 10(*b*)) can occur in D_2CO/D_2CO collisions with approximately gas-kinetic efficiency. It is possible to speculate that the small-$|\Delta J|$ propensity in K_a-changing RET reflects the role of the long-range dipole/dipole portion of the intermolecular potential. The efficiency of the large K_a-changes observed would then require the state-selected molecule to change its rovibrational energy by as much as $400\,cm^{-1}$, suggesting the possible involvement of rotational resonance effects (Oka 1967, 1973) in which the collision-partner D_2CO molecule undergoes a compensating change in K_a to keep the overall collision-induced process quasi-elastic.

Another inadequately studied topic which lends itself to the IRUVDR approach is that of 'K_c-changing RET' in D_2CO, with $|\Delta J| = |\Delta K_a| = 0$. This corresponds to RET from one component of an asymmetric-rotor doublet to another (Oka 1967, 1973). Several IRUVDR resonances lend themselves to studies of this kind, notably the $\nu_4/4_1^0$ excitation scheme involving the 10 P(16) CO_2-laser line (see table 1); preliminary investigations have been reported by Orr *et al.* (1981), but not with sufficient resolution or sensitivity to reach conclusions comparable to those obtained in the high-K_a region where asymmetric-rotor splitting is negligible (Orr *et al.* 1984, Bewick *et al.* 1988). The distinction between J-changing RET rates, in cases where asymmetry-doubling is and is not resolved, has been discussed by Bewick *et al.* (1988), together with a review of other experimental studies of RET in formaldehyde.

In the context of molecular excitation phenomena, Orr and Haub (1981) have proposed that a rotationally specific, collision-assisted sequence of infrared single-photon absorption steps might in favourable circumstances control the selective initial stage of infrared multiple-photon excitation in formaldehyde. The proposal is based on IRUVDR investigations of the $\tilde{A} \leftarrow \tilde{X}\, 4_2^1$ band of D_2CO, as depicted in figure 5. This provides a means of monitoring rovibrational population on the second 'rung' ($v_4 = 2$) of the vibrational ladder of D_2CO—a critical stage in infrared multiple-photon excitation. Cooperative laser excitation effects, assisted by collisions, have been found to produce marked departures from the populations expected on the basis of a single infrared absorption step within a thermally equilibrated vibrational manifold. The most extensive studies of this kind have been obtained with infrared excitation by the 10 P(14) CO_2-laser line, which has been shown under effectively collision-free conditions to yield 4_2^1-band IRUVDR signals *via* single-photon rovibrational pumping in the $2\nu_4 - \nu_4$ hot band, rather than two-photon pumping in the $2\nu_4$ band; detailed assignments are listed in table 1 (Orr and Haub 1981, 1984). Orr and Haub (1981) have performed IRUVDR experiments with relatively high D_2CO pressure (~ 1 Torr) and long CO_2-laser pulse duration ($\sim 1\,\mu s$) to demonstrate a collision-assisted excitation sequence of the following form: 10 P(14) CO_2-laser excitation of the $v_6 = 1$, $21_{1,20}$ rovibrational state; rapid collision-induced $\nu_6 \rightarrow \nu_4$ vibrational transfer and (J, K_a)-changing RET to odd-K_a states of the $v_4 = 1$ rovibrational manifold, populating states

such as $v_4 = 1, 8_{3,5}$ and $v_4 = 1, 9_{3,7}$; 10 P(14) CO_2-laser excitation of the $8_{4,5} \leftarrow 8_{3,5}$ and $9_{4,5} \leftarrow 9_{3,7}$ transitions in the $2\nu_4 - \nu_4$ hot band; (J, K_a)-changing RET to other even-K_a states of the $v_4 = 2$ rovibrational manifold. The first three steps are all supposed to take place within the one long CO_2-laser pulse, assisted by the relatively high sample pressure which promotes rotationally specific $\nu_6 \rightarrow \nu_4$ transfer of the type discussed in sections 6 and 7. The resulting IRUVDR signals indicate the establishment of rovibrational populations far in excess of what would be expected of a single infrared absorption step at thermal equilibrium. Assignment of the initial infrared absorption step in the ν_6 band remains tentative (Haub and Orr 1987).

A second example of a particularly efficient collision-assisted sequential excitation process involves the 10 P(16) CO_2-laser line, which has been studied by Haub (1985). Table 1 lists the single-photon resonances which have been identified under effectively collision-free conditions within the ν_4 and $2\nu_4 - \nu_4$ infrared bands. The 10 P(16) CO_2-laser line is believed to promote the following train of events: CO_2-laser excitation of the $v_4 = 1, 12_{3,10}$ rovibrational state; rapid collision-induced (J, K_a)-changing RET to other odd-K_a states of the $v_4 = 1$ rovibrational manifold, populating states such as $v_4 = 1, 10_{7,4}$ and $10_{7,3}$; CO_2-laser excitation of the $9_{8,2} \leftarrow 10_{7,4}$ and $9_{8,1} \leftarrow 10_{7,3}$ transitions in the $2\nu_4 - \nu_4$ hot band; further (J, K_a)-changing RET to other even-K_a states of the $v_4 = 2$ rovibrational manifold. Once again, the first three steps are all able to take place within the one long CO_2-laser pulse. Collisions in this instance are required only to assist (J, K_a)-changing RET, which has been shown recently by Bewick (1989) to be particularly efficient if $|\Delta K_a|$ is even and $|\Delta J|$ is small as in the present situation. The 10 P(16) CO_2-laser line therefore produces a particularly efficient multi-step process which does not need to invoke mode-to-mode (e.g. $\nu_6 \rightarrow \nu_4$) transfer, as was necessary in the previous 10 P(14) case (Orr and Haub 1981). Other more complicated collision-assisted excitation sequences involving the 10 P(20) and 10 P(24) CO_2-laser lines have been studied (Orr and Haub 1981, Haub 1985). There are elements of speculation in the assignment of some of these processes, but they do suggest how judicious choice of infrared wavelength and collisional conditions can transfer a substantial proportion of rovibrational population from the $v = 0$ ground state to higher levels of the vibrational ladder. Moreover, limited rotational selectivity appears to be attainable, owing to the tendency for collision-induced $\nu_6 \rightarrow \nu_4$ vibrational transfer and (J, K_a)-changing RET to proceed through a limited range of rotationally specific channels. The laser photochemical implications of such processes have not yet adequately been explored.

This review has been deliberately introspective, in order to concentrate the reader's attention on the spectroscopic details and energy transfer processes revealed by our time-resolved IRUVDR experiments. A disadvantage of this approach is that it has not done justice to the immense body of supporting scientific literature on which this work has depended. Much of the relevant literature has been referenced in our published papers, the following of which contain particularly extensive reviews: Orr and Nutt (1980b), Orr and Haub (1984), Haub and Orr (1987), Orr and Smith (1987), Bewick *et al.* (1988). The comprehensive reviews by Clouthier and Ramsay (1983) and by Moore and Weisshaar (1983), dealing with the spectroscopy and photochemistry of formaldehyde, are also useful in this regard. Nevertheless, there are a number of contributions from other research groups which merit a specific listing here (together with some representative literature references), in view of the valuable stimulus which they have given to our own research programme: the pioneering work of Oka (1967, 1973) on microwave–microwave double resonance studies of RET in several polyatomic

molecules, including formaldehyde; the extensive overtone-excitation studies of rotational and vibrational energy transfer in HF(g) by Crim and co-workers, which have provided a diatomic 'template' for much of our progress in understanding polyatomic rovibrational energy transfer in formaldehyde (Copeland *et al.* 1982, 1983, Copeland and Crim 1983, 1984, Jursich *et al.* 1984, Robinson *et al.* 1986); intensive exploration of the photophysics of formaldehyde in its excited electronic state, by groups such as those of Moore (Moore and Weisshaar 1983, Guyer *et al.* 1986, Polik *et al.* 1988), Lee (Apel and Lee 1984, 1985, Garland *et al.* 1983, 1986) and Schlag (Henke *et al.* 1982a, b, Schlag *et al.* 1982); infrared double-resonance studies of *J*- and *K*-changing RET in polyatomic molecules, parallel to our own work on formaldehyde, by Steinfeld and co-workers (Harradine *et al.* 1984, Foy *et al.* 1988); the wide variety of innovative experiments performed by Field, Kinsey and co-workers, particularly those investigating formaldehyde in high levels of rovibrational excitation (Dai *et al.* 1985a, b, Temps *et al.* 1987, 1988) and those studying RET (Temps *et al.* 1987, Vaccaro *et al.* 1988); a vast body of work on intramolecular energy transfer processes in congested rovibronic manifolds of large polyatomic molecules, well represented by the contributions of Parmenter (1982, 1983); an equally vast body of literature on infrared multiphoton excitation and laser-assisted photochemistry (Fuss and Kompa 1981, King 1982, Quack, 1982); the work of theoreticians such as Alexander (1982; Pouilly *et al.* 1984), Clary (1987; Peet and Clary, 1986), Freed (1981, 1984) and Parson (1988, 1989, 1990), which has helped us to interpret some of the unusual phenomena observed in formaldehyde. Much of this work by other groups has evolved in parallel with our own, providing many rewarding scientific interchanges.

Acknowledgments

The final task of this review is to acknowledge valuable contributions to the progress of the work described, by various research students and colleagues. Three people deserve to be singled out for primary credit: Dr Gary Nutt, whose skill and perseverence was the key to our initial success in IRUVDR experiments (see section 3), and Drs John Haub and Chris Bewick, whose respective Ph.D. research projects have revealed many of the mysteries of formaldehyde (and have left us wondering about others). Special mention must also be made of Drs Ron Haines and Joe Martins, for their contributions on the computational and kinetic modelling front. Others who have been active in our investigations of IRUVDR in formaldehyde include Drs Jim Steward, Frank Duarte and Ben Duval (all working as postdoctoral fellows), as well as B.Sc. Honours students Os Vozzo and Robert Hynes. Interest and support from numerous colleagues around the world, particularly those at NRCC Ottawa (where, as section 3 reveals, the story began), is also much appreciated. The continual financial support by the Australian Research Grants Scheme (now the Australian Research Council), by the University of New South Wales and (since 1988) by Macquarie University are also gratefully acknowledged.

References

ALEXANDER, M. H., 1982, *J. chem. Phys.*, **76**, 429.
APEL, E. C., and LEE, E. K. C., 1984, *J. phys. Chem.*, **88**, 1283; 1985, *Ibid.*, **89**, 1391.
BEWICK, C. P., 1989, Ph.D. Thesis, University of New South Wales.
BEWICK, C. P., DUVAL, A. B., and ORR, B. J., 1985, *J. chem. Phys.*, **82**, 3470.
BEWICK, C. P., HAUB, J. G., HYNES, R. G., MARTINS, J. F., and ORR, B. J., 1988, *J. chem. Phys.*, **88**, 6350.

BEWICK, C. P., and ORR, B. J., 1989a, *Chem. phys. Lett.*, **159,** 66; 1989b, *Ibid.*, **159,** 73.
BRAND, J. C. D., 1956, *J. chem. Soc. Lond.*, 858.
BRUNNER, T. A., and PRITCHARD, D., 1982, *Adv. chem. Phys.*, **50,** 589.
BUNKER, P. R., 1979, *Molecular Symmetry and Spectroscopy* (New York: Academic).
CHADWICK, B. L., KING, D. A., BERZINS, L., and ORR, B. J., 1989, *J. chem. Phys.*, **91,** 7994.
CLARY, D. C., 1987, *J. phys. Chem.*, **91,** 1718.
CLOUTHIER, D. J., and RAMSAY, D. A., 1983, *Ann. Rev. phys. Chem.*, **34,** 31.
COPELAND, R. A., and CRIM, F. F., 1983, *J. chem. Phys.*, **78,** 5551; 1984, *Ibid.*, **81,** 5819.
COPELAND, R. A., PEARSON, D. J., ROBINSON, J. M., and CRIM, F. F., 1982, *J. chem. Phys.*, **77,** 3974; 1983, *Ibid.*, **78,** 6344.
DAI, H.-L., KORPA, C. L., KINSEY, J. L., and FIELD, R. W., 1985a, *J. chem. Phys.*, **82,** 1688.
DAI, H.-L., FIELD, R. W., and KINSEY, J. L., 1985b, *J. chem. Phys.*, **82,** 2161.
DUVAL, A. B., KING, D. A., HAINES, R., ISENOR, N. R., and ORR, B. J., 1985, *J. opt. Soc. Am.* B, **2,** 1570; 1986, *J. Raman Spectrosc.*, **17,** 177.
EBERS, E. S., and NIELSEN, H. H., 1938, *J. chem. Phys.*, **6,** 311.
FOY, B., HETZLER, J., MILLOT, G., and STEINFELD, J. I., 1988, *J. chem. Phys.*, **88,** 6838.
FREED, K. F., 1981, *Photoselective Chemistry*, Part 2, edited by J. Jortner (New York: Wiley), p. 291; 1984, *Chem. phys. Lett.*, **106,** 1.
FUSS, W., and KOMPA, K. L., 1981, *Prog. quant. Electron.*, **7,** 117.
GARLAND, N. L., and LEE, E. K. C., 1983, *Faraday Discuss. chem. Soc.*, **75,** 377; 1986, *J. chem. Phys.*, **84,** 28.
GUYER, D. R., POLIK, W. F., and MOORE, C. B., 1986, *J. chem. Phys.*, **84,** 6519.
HANSCH, T. W., 1972, *Appl. Optics*, **11,** 895.
HARRADINE, D., FOY, B., LAUX, L., DUBS, M., and STEINFELD, J. I., 1984, *J. chem. Phys.*, **81,** 4267.
HAUB, J. G., 1985, Ph.D. Thesis, University of New South Wales.
HAUB, J. G., and ORR, B. J., 1984, *Chem. phys. Lett.*, **107,** 162; 1987, *J. chem. Phys.*, **86,** 3380.
HENKE, W. E., SELZLE, H. L., HAYS, T. R., SCHLAG, E. W., and LIN, S. H., 1982a, *J. chem. Phys.*, **76,** 1327; 1982b, *Ibid.*, **76,** 1335.
HERZBERG, G., 1966, *Molecular Spectra and Molecular Structure. III. Electronic Spectra and Electronic Structure of Polyatomic Molecules* (Princeton: Van Nostrand).
JOB, V. A., SETHURAMAN, V., and INNES, K. K., 1969, *J. molec. Spectrosc.*, **30,** 365.
JURSICH, G. M., RITTER, D. R., and CRIM, F. F., 1984, *J. chem. Phys.*, **80,** 4097.
KING, D. S., 1982, *Adv. chem. Phys.*, **50,** 105.
KING, D. A., HAINES, R., ISENOR, N. R., and ORR, B. J., 1983, *Optics Lett.*, **8,** 629.
MCCAFFERY, A. J., PROCTOR, M. J., and WHITAKER, B. J., 1986, *Ann. Rev. phys. Chem.*, **37,** 223.
MOORE, C. B., and WEISSHAAR, J. C., 1983, *Ann. Rev. phys. Chem.*, **34,** 525.
OKA, T., 1967, *J. chem. Phys.*, **47,** 13; 1973, *Adv. atomic molec. Phys.*, **9,** 127.
ORR, B. J., 1974, *Spectrochim. Acta*, **80,** 1275.
ORR, B. J., and NUTT, G. F., 1980a, *Optics Lett.*, **5,** 12; 1980b, *J. molec. Spectrosc.*, **84,** 272.
ORR, B. J., and HAUB, J. G., 1981, *Optics Lett.*, **6,** 236; 1984, *J. molec. Spectrosc.*, **103,** 1.
ORR, B. J., HAUB, J. G., and HAINES, R., 1984, *Chem. phys. Lett.*, **107,** 168.
ORR, B. J., HAUB, J. G., NUTT, G. F., STEWARD, J. L., and VOZZO, O., 1981, *Chem. phys. Lett.*, **78,** 621.
ORR, B. J., and SMITH, I. W. M., 1987, *J. phys. Chem.*, **91,** 6106.
PARMENTER, C. S., 1982, *J. phys. Chem.*, **86,** 1735; 1983, *Faraday Discuss. chem. Soc.*, **75,** 7.
PARSON, R., 1988, *Chem. phys. Lett.*, **145,** 211; 1989, *J. chem. Phys.*, **91,** 2206; 1990, *Ibid.*, **92,** 304.
PEET, A. C., and CLARY, D. C., 1986, *Molec. Phys.*, **59,** 529.
POLIK, W. F., MOORE, C. B., and MILLER, W. H., 1988, *J. chem. Phys.*, **89,** 3584.
POUILLY, B., ROBBE, J. M., and ALEXANDER, M. H., 1984, *J. phys. Chem.*, **88,** 140.
QUACK, M., 1982, *Adv. chem. Phys.*, **50,** 395.
ROBINSON, J. M., RENSBERGER, K. J., and CRIM, F. F., 1986, *J. chem. Phys.*, **84,** 220.
SCHLAG, E. W., HENKE, W. E., and LIN, S. H., 1982, *Int. Rev. phys. Chem.*, **2,** 43.
STEINFELD, J. I., and HOUSTON, P. L., 1978, *Laser and Coherence Spectroscopy*, edited by J. I. Steinfeld (New York: Plenum), chapter 1.
STRICKLER, S. J., and BARNHART, R. J., 1982, *J. phys. Chem.*, **86,** 448.
TEMPS, F., HALLE, S., VACCARO, P. H., FIELD, R. W., and KINSEY, J. L., 1987, *J. che. Phys.*, **87,** 1895; 1988, *J. chem. Soc., Faraday Trans.* II, **84,** 1457.
VACCARO, P. H., TEMPS, F., HALLE, S., KINSEY, J. L., and FIELD, R. W., 1988, *J. chem. Phys.*, **88,** 4819.
WEITZ, E., and FLYNN, G., 1981, *Adv. chem. Phys.*, **47,** 185.
YARDLEY, J. T., 1980, *Introduction to Molecular Energy Transfer* (New York: Academic).